A STUDY OF RADIO FREQUENCY INTERFERENCE TO AUTOMOTIVE RADIO SYSTEMS

by

Joseph E. Ferris and Dipak L. Sengupta
The Radiation Laboratory
Department of Electrical and Computer Engineering
University of Michigan
Ann Arbor, Michigan 48109

Final Report

1 September 1978 to 31 December 1979

August 1980

Purchase Order No. 47-J-546918

Prepared for

Ford Motor Company
Electrical and Electronics Division
Radio and Speed Control Engineering Dept.
EEE Building, Room A170
Dearborn, Michigan 48121

320892-1-F = RL-2530

A STUDY OF RADIO FREQUENCY INTERFERENCE TO AUTOMOTIVE RADIO SYSTEMS

FINAL REPORT

Purchase Order No. 47-J-546918

1 September 1978 to 31 December 1979

August 1980

Prepared by: Joseph E. Ferris and Dipak L. Sengupta

Prepared for: Electrical and Electronics Division
Ford Motor Company
Radio and Speed Control Engineering Department
EEE Building, Room A170
Dearborn, Michigan 48121

EXECUTIVE SUMMARY

Radio Frequency Interference (RFI) to automotive radio systems has been studied by measuring the vehicle ignition system-generated RFI signals at the radio terminals of the car, and by measuring the response of test radios to laboratory-generated RF carrier plus short pulse input signals. In addition, the use of field probes or sensors was explored to measure and quantify the vehicle ignition system generated RFI signals existing on or near the vehicle surface. The test vehicles used were: 1977 Chevrolet Monte Carlo, 1978 Mercury Cougar and 1979 Ford LTD. The eleven test radios used were typical of those in Ford-built automobiles.

The vehicle ignition system-generated RFI signals at its entertainment radio antenna terminals have been measured in time and frequency domain. In general, it has been found that the received signals in the time domain are pulsed in nature, and very little correlation has been observed between two or more received pulses. Frequency components of a received pulse have been measured in the range 20 to 1000 MHz; the measured frequency spectrum (i.e., amplitude of the frequency component vs. frequency) has been correlated with that of a typical ignition pulse.

It has been found that the front mounted antennas receive more RFI signals than the rear mounted antennas; windshield and front mounted antennas on the same car receive RFI signals having the same order of magnitude. RFI signals received at the antenna terminals of Ford cars ranged between 20 to 40 mv, while with the competitor car the received RFI signal was 400 mv.

Although the response of radio systems to RFI signals was studied with controlled input signals in a laboratory atmosphere, the results obtained can be used to estimate the vulnerability of these radios to such signals in an actual automotive environment. It has been found that the response of a radio to impulse signals depends significantly on the RF carrier signal amplitude at the radio input terminals--generally, an existing RF carrier tends to reduce the overall interference effects of the pulse. The pulse response of a radio does not depend significantly on the pulse repetition rate but is affected quite strongly by the pulse width. Simple Fourier analysis techniques have been used to correlate the response of a radio to the frequency spectrum of the input pulse. All radios tested appear to respond similarly to similar input signals--no significant difference in performance has been observed from radio to radio for the same RF carrier plus short pulse input signals.

On the basis of the results obtained, it has been established that with a given level of RF carrier signal at the input terminals, an input short pulse signal (similar to vehicle ignition system generated RFI signal) of amplitude 3650 times larger (i.e., 71 dB larger) than that of the RF carrier will produce threshold audio noise at the output of the radios. Of course, input pulses having larger amplitude will produce larger noise output. The above number can be used to estimate the vulnerability of a given radio system to RFI signals.

Measurements of the vehicle-generated RFI fields on or near the vehicle surface indicate that it is possible to measure and quantify the RFI signals using electrostatically shielded circular loops. On the

basis of the results obtained, it is recommended that the RFI signals on or near the vehicle surface be measured with one- or three-inch diameter loops, respectively.

TABLE OF CONTENTS

I. INTRODUCTION

It is well-known [1] that the primary sources of Radio Frequency Interference (RFI) to automotive radio systems are the impulse noises (or the short electromagnetic pulses) generated by the vehicle ignition system itself and coupled, predominantly by radiation mechanisms [2], to the radio antenna. The present investigation has been directed towards a better understanding of the vehicle generated interference signals at the entertainment radio antenna terminals, and their effects on the radio reception in the presence of these signals. In particular, the investigation consisted of three major parts: (i) investigation of the ignition generated signals at the output terminals of the radio antenna, (ii) measurement of the susceptibility of the radio to impulsive noise signals, and (iii) application of field sensors or probes for measuring the fields on or near the vehicle surface created by the vehicle ignition system.

With the test vehicle engine running at its idle speed ($\sim$1000 rpm), the signals at the output terminals of the antenna have been measured in the time domain using an oscilloscope, and in the frequency domain using a spectrum analyzer. The objective of these measurements has been to determine the appropriate characteristics of the vehicle generated RFI signals (at the radio input) which can later be correlated to its radio output. The test vehicles used were 1977 Chevrolet Monte Carlo, 1978 Mercury Cougar and 1979 Ford LTD. The Monte Carlo used a windshield antenna; both windshield and triband antennas were used on the Cougar, and only a triband antenna was used on the Ford LTD. All these antennas were mounted at their usual locations on the test vehicles. Various results obtained are described in Chapter II.

Susceptibility of the test radios to impulse noise signals has been studied inside an electrically screened room and using laboratory generated signals. The test radio was initially set to standard test conditions. Measurements were carried out with laboratory generated impulsive and RF carrier signals directly coupled to the RF input of the radio. The response of a radio to the input short pulses was measured with and without RF signals applied to the input. The susceptibility characteristics of the radio to impulsive noise signals were determined by tuning the radio to several frequencies within the FM broadcast band and by adjusting the level of the imput pulse signals until perceptible audio interference was obtained at the output. Fourier analysis techniques were then used to interpret various results obtained. The results indicate that there is a fixed input RF carrier to pulse signal amplitude ratio below which the radio reception would experience appreciable interference due to the pulse. Discussion and analysis of various results obtained are discussed in Chapter III.

The possible use of field probes or sensors to obtain repeatable measurements of the vehicle ignition system generated electromagnetic fields on or near the vehicle surface has been investigated. Two electrostatically shielded loops have been fabricated and used as field probes or sensors to measure the RFI fields generated by the ignition system of a Ford LTD. The results are described in Chapter IV.

II. INVESTIGATION OF THE RFI SIGNAL AT THE RADIO ANTENNA TERMINALS

The RFI signals originating from the automobile ignition system and received by its entertainment radio antenna have been studied experimentally both in the time and frequency domain. Before discussing the results it is appropriate to describe the techniques used for collecting various data.

2.1 Measurement Techniques

2.1.1 Time Domain. The time domain measurements were carried out by using the test set-up shown in Fig. 1. Three oscilloscopes, all manufactured by Tektronix, were used during various phases of the measurement: they were Model No. 465, 7623A, and 7834 with a 7A16 vertical amplifier and 7085 delay time base. The last named oscilloscope (i.e., 7834) was obtained on loan from Ford Scientific Laboratories and was available for a limited time only. The oscilloscope Model 465 was found unsuitable for the present time domain measurement because of its slow writing speed and the low repetition rate of the ignition pulses. After considerable experimentation it was learned that the most meaningful data could be obtained by using the following procedure:

(i) Sample the ignition pulse, fed to a particular spark plug, by means of a capacitor coupling clamp attached to the plug wire. Use this pulse as the sync trigger for the oscilloscope.

(ii) Connect the output of the automobile entertainment radio antenna to the vertical input of the oscilloscope.

(iii) Using the single sweep mode of the oscilloscope observe, on its screen, the received signal due to the ignition pulse used in (i).

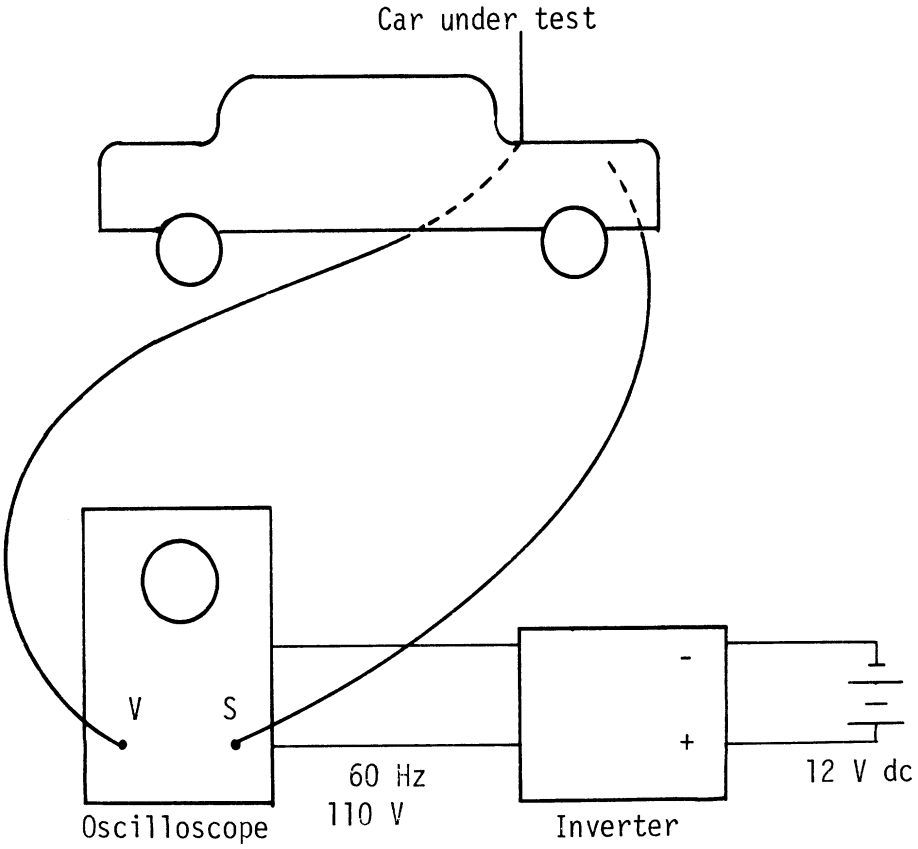

Figure 1. Test set-up for time domain measurement.

(iv) As a permanent record, take a polaroid picture of the signal received in (iii).

(v) Repeat (i)-(iv) for signals originating from different spark plugs.

2.1.2 Frequency Domain. Figure 2 shows the experimental arrangement used during the frequency domain measurement. The spectrum analyzer used was Tektronix Model 7633/7L13 which covered the range of frequencies 1 kHz to 1.8 GHz. This particular model of spectrum analyzer was used because it has a variable persistency option which allows the operator to store data on its oscilloscope-screen for a period of time so that the entire trace can be seen, and then photographically record the data for later analysis. The test set-up shown in Fig. 2 is quite simple to use; all that is needed is to connect the output of the automobile entertainment antenna to the input of the spectrum analyzer.

With the above set-up and with the test vehicle engine on and off, data were collected over 100 MHz bands within the frequency range 0 - 1 GHz. Comparing the two sets of results within each band, the frequency components of the received RFI signal originating from the automobile ignition system were identified. Of course, the present method precludes the identification of those frequency components of the interfering signal which are coincident with the frequency components of the ambient signals received from outside.

2.2 Test Vehicles

Results were obtained by using the three test vehicles with receiving antennas, as noted in Table 1.

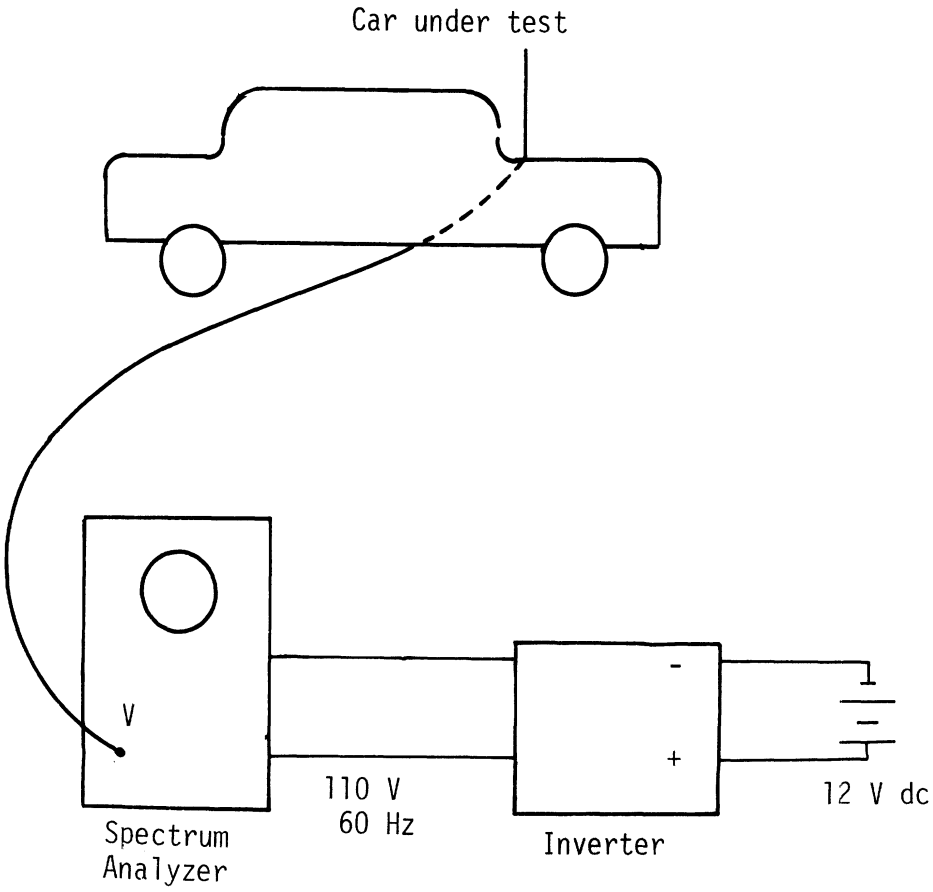

Figure 2. Test set-up for frequency domain measurement.

Table 1

Test Vehicles and Associated Antennas

Test Vehicle	Receiving Antenna
1977 Chevrolet Monte Carlo	Windshield
1978 Mercury Cougar	Windshield Power Tri-band (left,rear) Manual Tri-band (right, front)
1979 Ford LTD	Manual Tri-band (right, front)

The first two vehicles (Monte Carlo and Cougar) were supplied by Ford Motor Co., and the third (Ford LTD) was leased from a local Ford dealer. All three vehicles had eight-cylinder engines; the Monte Carlo and LTD had 305 cubic inch engines. The windshield antenna on the Monte Carlo was a standard receiving antenna installed by the manufacturer; the windshield antenna on the Cougar was an experimental receiving antenna supplied by Ford and installed by us. Both the power and manual tri-band antennas were standard entertainment antennas built by Ford.

2.3 Signals Received by the Radio Antenna

The present section discusses various results characterizing the received signals as functions of time and frequency.

2.3.1 Time Domain. With the engine of each test vehicle running at an idle-speed of about 1000 rpm, the ignition generated RFI signals at the terminals of the vehicle entertainment antenna have been measured as functions of time using the test set-up of Fig. 1. Typical photographs of the received signals obtained with the three vehicles are

shown in Fig. 3. The results indicate that the competitors car (Monte Carlo) provides the largest (peak-to-peak) received signal. Typically, the peak-to-peak amplitude of the signal recieved with the competitor car was about 400 mV whereas those of the signals received with the Ford cars ranged from 20 mV to 40 mV. We do not have any explanation for this except that it may be due to the increased strength of the ignition pulses generated by the competitor car.

The Cougar results (Fig. 3b,c,d) indicate that the distance of the antenna from the RFI signal source (i.e., the spark plug region where the ignition pulse originates) plays a significant role in determining the amplitude of the received signal. For example, the rear antenna, being farthest from the engine, received the smallest amplitude signal whereas the front antenna, being nearest, received the strongest signal. It can also be seen from Fig. 3 that the signal recieved with Ford LTD is of smaller amplitude than that received by the front-mounted tri-band antenna on Cougar; this is probably due to the fact that the engine-to-antenna distance is larger for the LTD.

It is known [1,3] that the automobile ignition system generated electromagnetic pulse is typically 10 ns long and that it contains a large number of frequency components ranging from DC to several hundred MHz [1,2]. An examination of the results shown in Fig. 3 reveals that the envelopes of the received signals are generally pulsed in nature, and that all the received signals exhibit a ringing phenomenon in time at a predominant frequency of about 100 MHz. This is due to the fact that the entertainment antennas are designed to be resonant at a nominal frequency of 100 MHz, and consequently the antenna tends to reject the

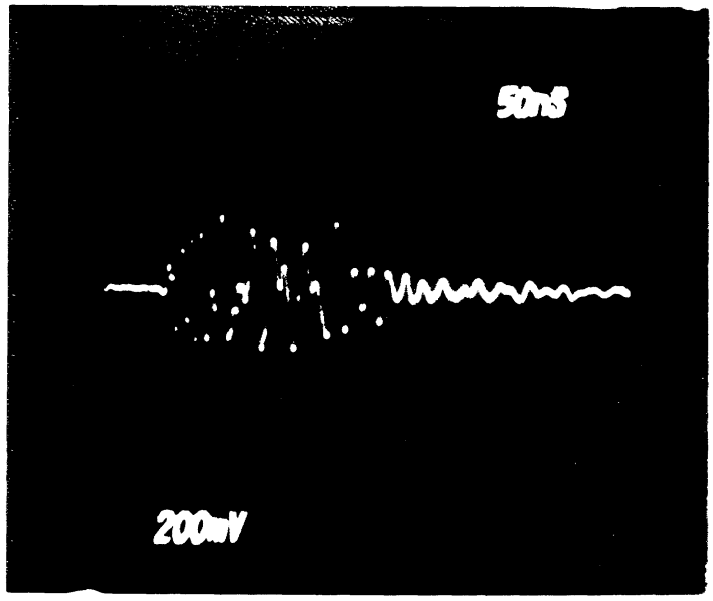

200 mV/division

50 ns/division

(a) Monte Carlo with windshield antenna.

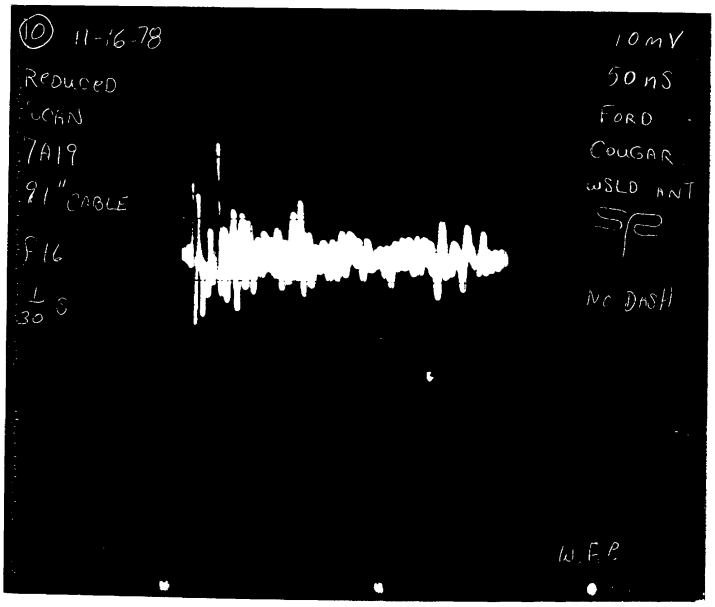

10 mV/division

50 ns/division

(b) Cougar with windshield antenna.

Figure 3. Time domain signals received at the antenna terminals of test cars

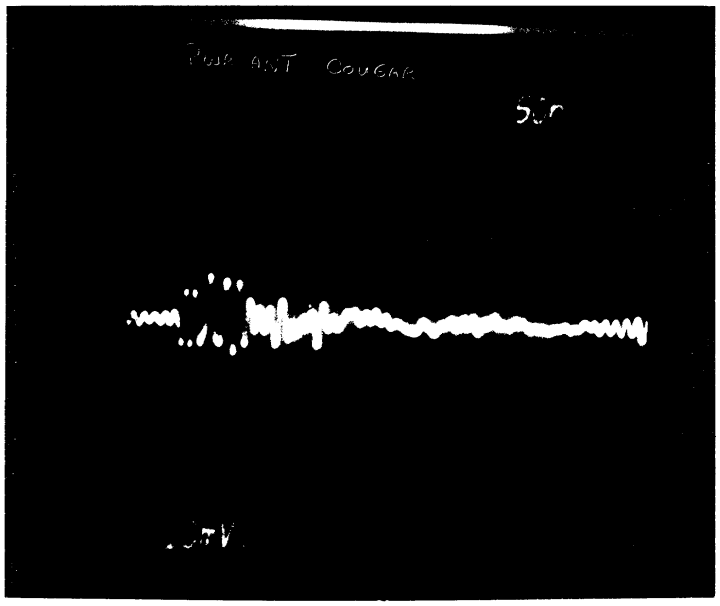

50 ns/division

(c) Cougar with power tri-band (rear mounted) antenna.

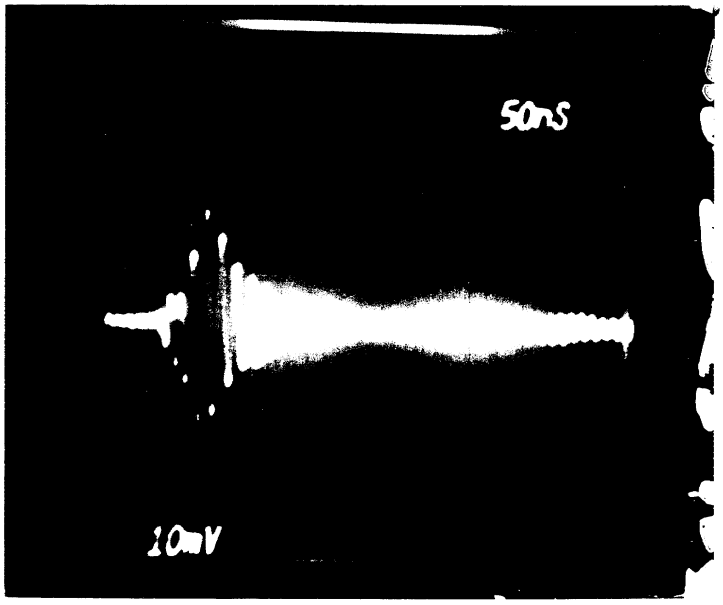

50 ns/division

(d) Cougar with manual tri-band (front mounted) antenna.

Figure 3. (continued). Time domain signals recieved at the antenna terminals of test cars.

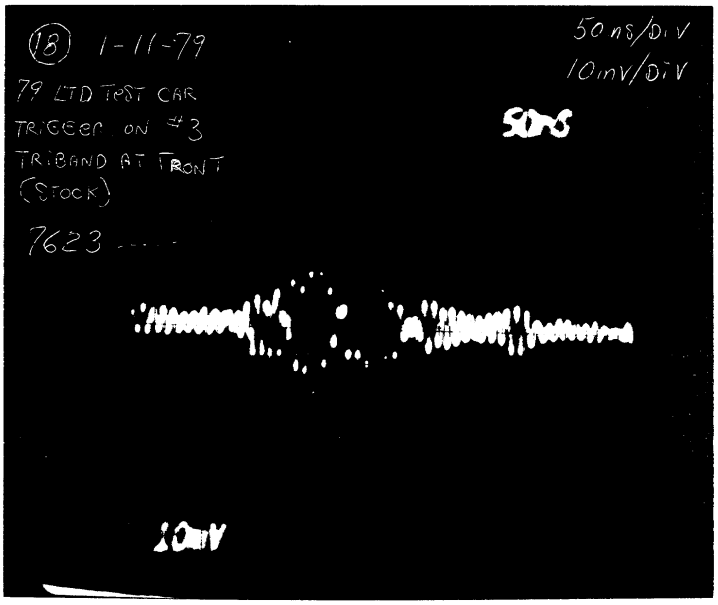

10 mV/division

50 ns/division

(e) Ford LTD with manual tri-band (front mounted) antenna

Figure 3. (continued). Time domain signals received at the antenna terminals of test cars.

lower frequency components and accept mainly the frequency components near the resonant frequency and, possibly, its harmonics which accounts for the slight increase of frequency of the received signal during the latter parts of the on-time received signals in Fig. 3.

Figures 4a,b,c show the received signals originating from the engine cylinder Nos. 7, 5 and 3, respectively, of the Ford LTD. Although the received signals in the three cases exhibit the same ringing frequency (~100 MHz), the amplitude and shape of the received pulse differ from cylinder to cylinder. The pulse shape variation may be due to the fact that each cylinder employs a different length of ignition wire. The cylinder No. 3 is located farthest from the antenna (see Fig. 5) and also it is significantly shielded by the engine; this would account for the smallest amplitude signal received by the antenna as shown in Fig. 4c.

The results discussed above are typical of received signals due to the initial electromagnetic pulse generated by the automobile ignition system. During discussion with the personnel of Ford Scientific Laboratories [3] it was learned that there is often a second pulse following the initial pulse. This can be seen in Fig. 6 which gives the signal received with Ford LTD for a sufficient length of time, to show the received signal due to the second ignition pulse also (compare with Fig. 3e). It should be noted that the two pulses in Fig. 6 are separated in time by approximately 1.5 μsec which is far less than the time of separation between the adjacent cylinder firings (nominally 0.015 sec for idle-speed ~1000 rpm).

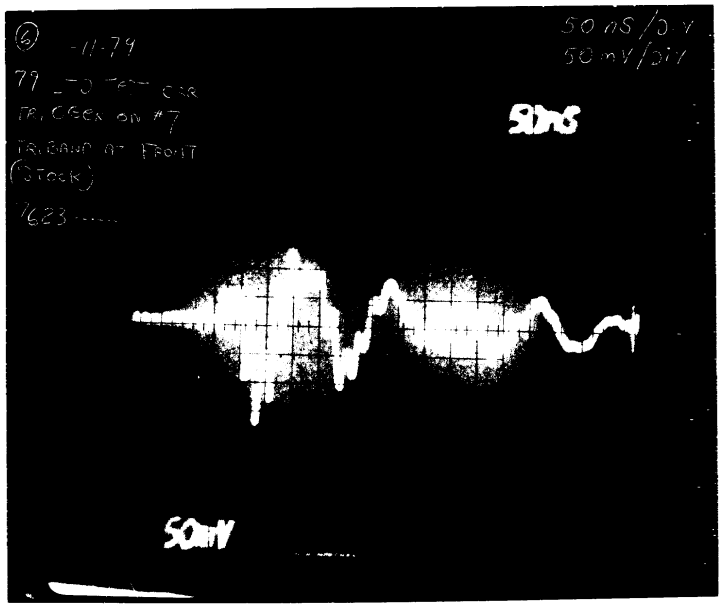

50 mV/division

50 ns/division

(a) Cylinder No. 7.

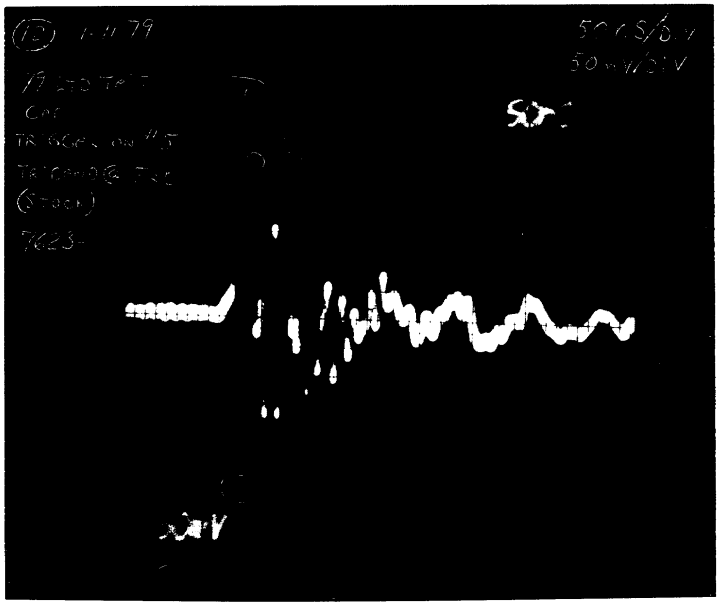

50 mV/division

50 ns/division

(b) Cylinder No. 5.

Figure 4. Received time domain signals originating from the individual engine cylinders of Ford LTD.

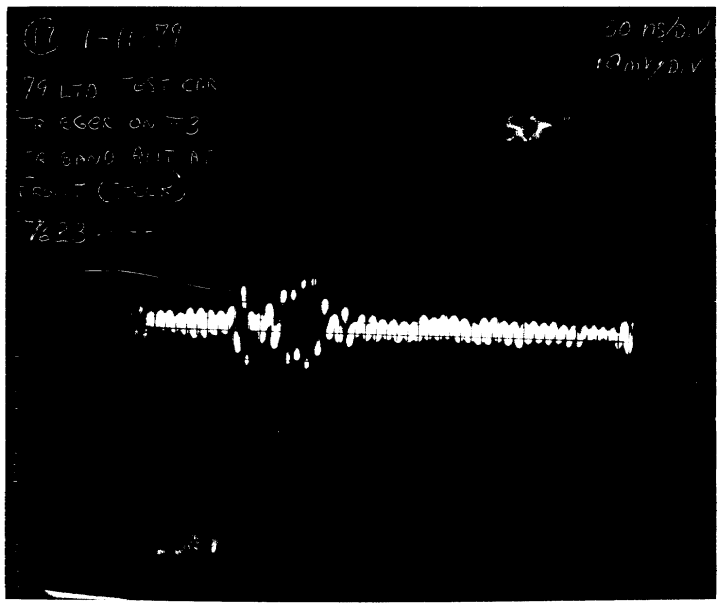

10 mV/division

50 ns/division

(c) Cylinder No. 3.

Figure 4. (continued). Received time domain signals originating from individual engine cylinders of Ford LTD.

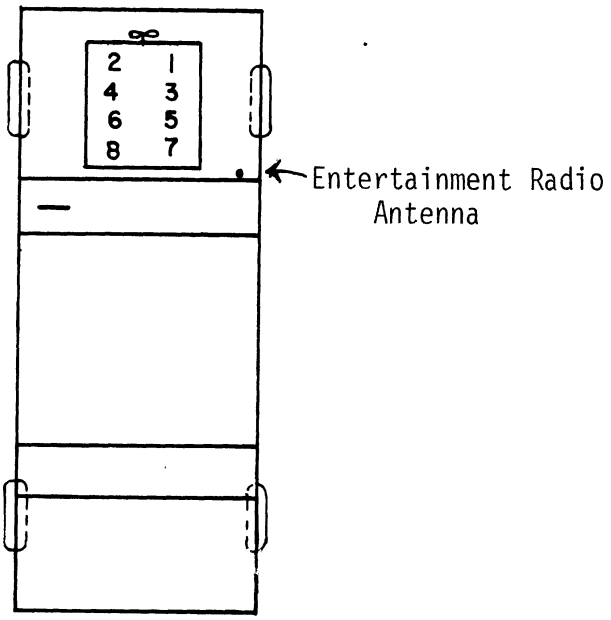

Figure 5. Location of the engine cylinders and the entertainment radio antenna.

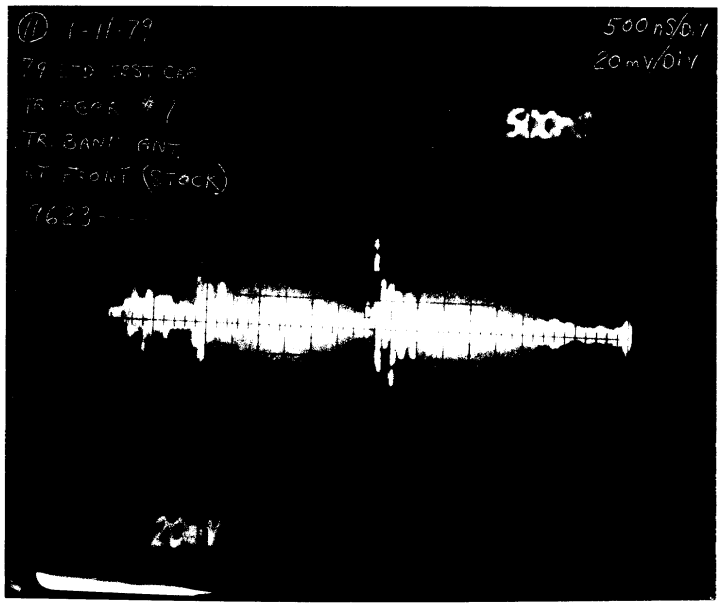

20 mV/division

500 ns/division

Figure 6. Received time domain signals with Ford LTD, showing the effect of the second ignition pulse.

It is worth noting that a comparison of two or more received pulses, originating from the firings of a particular cylinder, indicated that they were only vaguely similar. There was considerably less similarity between the received signals originating from the firings of the adjacent cylinders. In this sense, the received ignition noise signals are, generally, random in time.

2.3.2 Frequency Domain. Frequency domain results were obtained using the test set-up shown in Fig. 2. Typical results obtained with Ford LTD are shown in Figs. 7(a-h, a'-h') where the set of results a-h and a'-h' were obtained with the vehicle engine on and off, respectively, and where the results are shown in 100 MHz bands over the frequency range 0 - 100 MHz. Within each band of frequencies, the received signal components originating from the auto ignition system may be identified by comparing the results obtained with the engine on and off. For example, the results clearly indicate the existence of the following frequency components in the received signal originating from the ignition system of Ford LTD: 70, 120, 240, 370, 440, 620 and 740 MHz. Figure 8 shows the amplitude of the received signal frequency components as a function of frequency; it is clear from Fig. 8 that the amplitude of a frequency components of the received signal generally agree with those obtained from Fourier analysis of the train of short pulses similar to the ignition generated pulses (see Fig. 13 discussed later). However, it should be noted that before reaching the antenna the RFI signal will suffer attenuation due to the following: shielding by the engine and carburetor etc., space attenuation over the ignition pulse source-to-the antenna. The

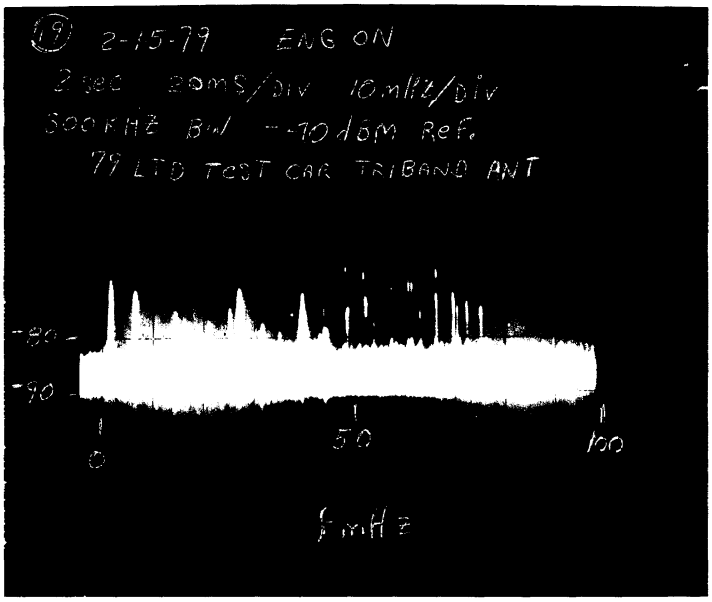

-10 dBm/division

10 MHz/division

(a) 0 to 100 MHz; Engine on.

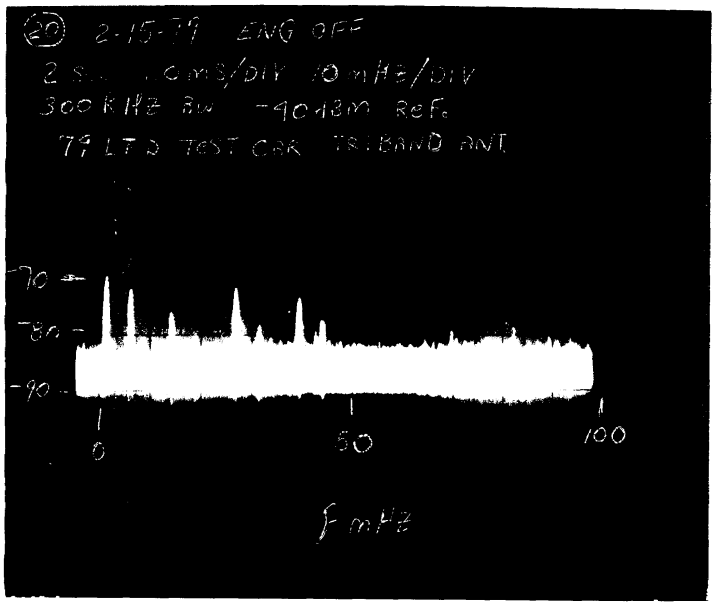

-10 dBm/division

10 MHz/division

(a') 0 to 100 MHz; Engine off.

Figure 7. Frequency domain signals obtained with Ford LTD.

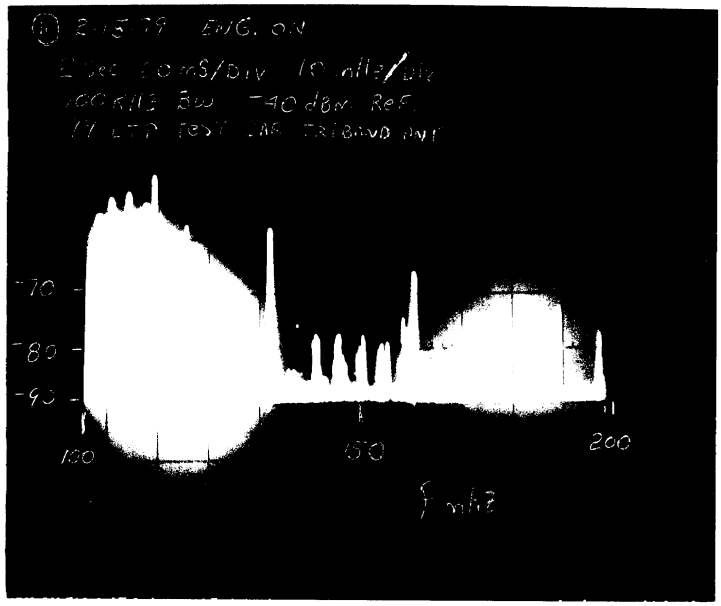

-10 dBm/division

10 MHz/division

(b) 100 to 200 MHz; Engine on.

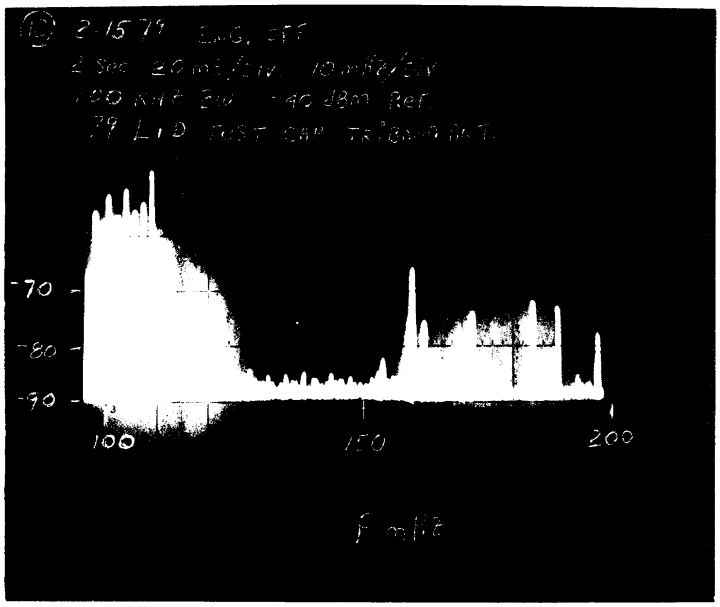

-10 dBm/division

10 MHz/division

(b') 100 to 200 MHz; Engine off.

Figure 7. (continued). Frequency domain signals obtained with Ford LTD.

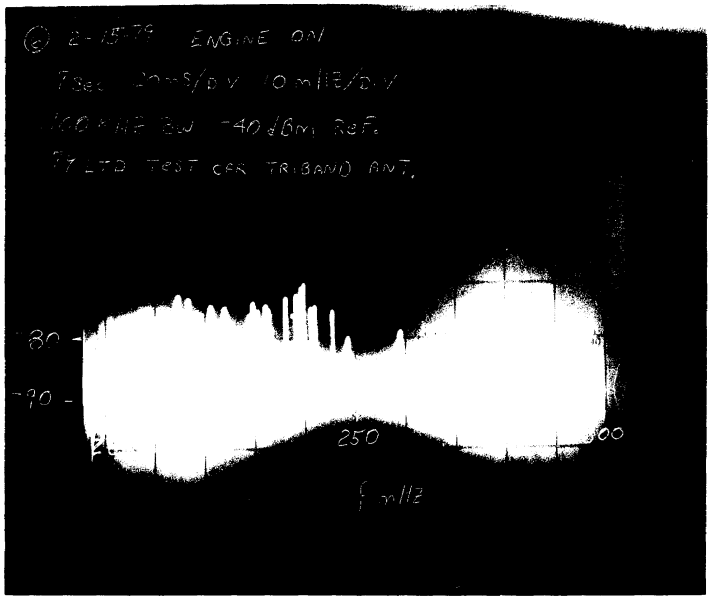

-10 dBm/division

10 MHz/division

(c) 200 to 300 MHz; Engine on.

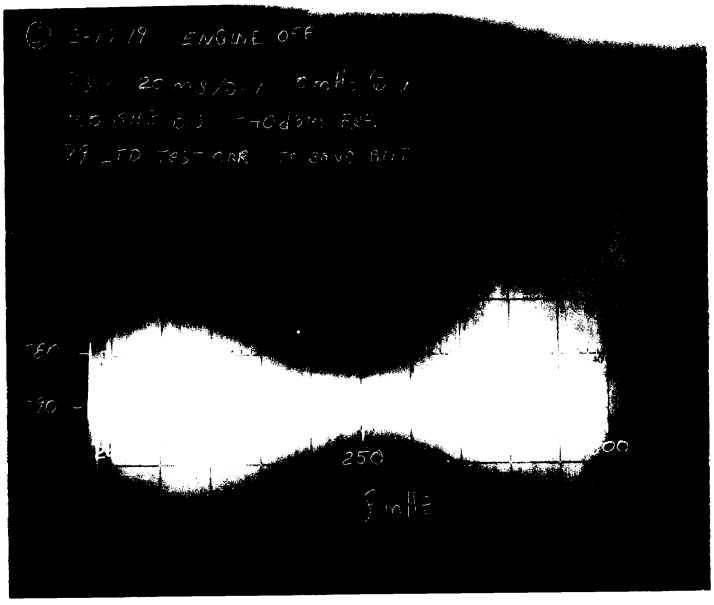

-10 dBm/division

10 MHz/division

(c') 200 to 300 MHz; Engine off.

Figure 7. (continued). Frequency domain signals obtained with Ford LTD.

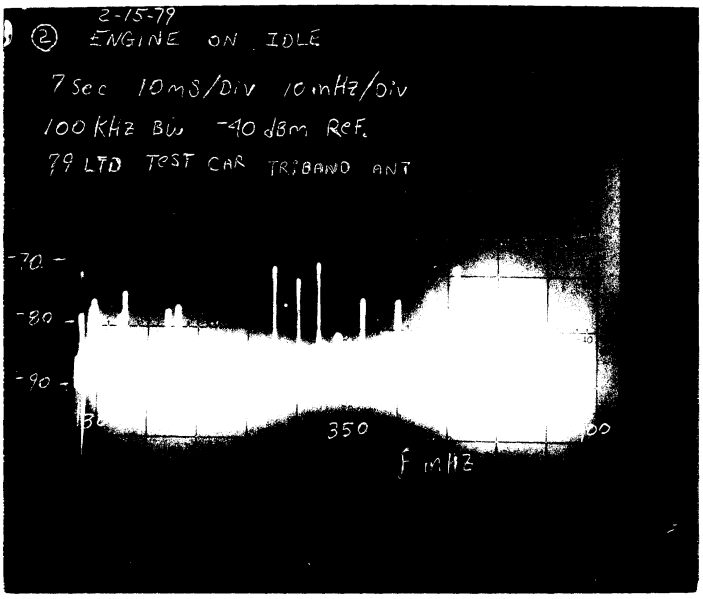

10 dBm/division

10 MHz/division

(3) 300 to 400 MHz: Engine on.

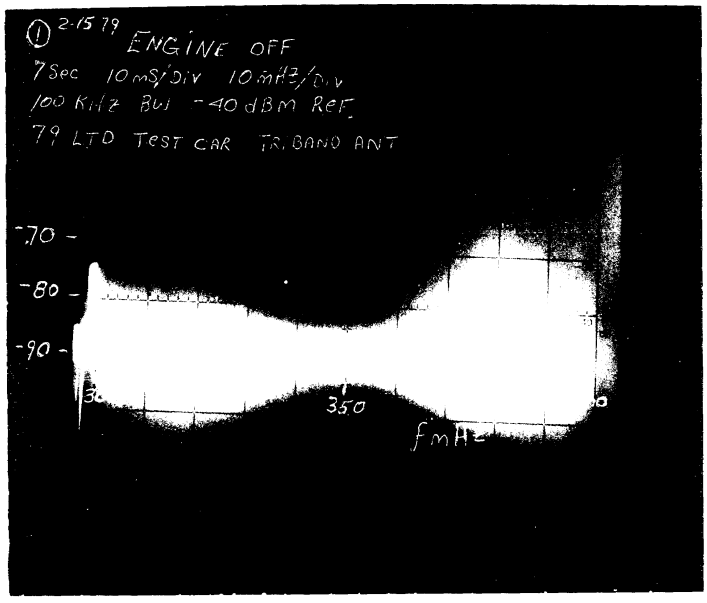

10 dBm/division

10 MHz/division

(4) 300 to 400 MHz. Engine off.

Figure [illegible] (cont'd). Frequency domain signal obtained with Ford LTD.

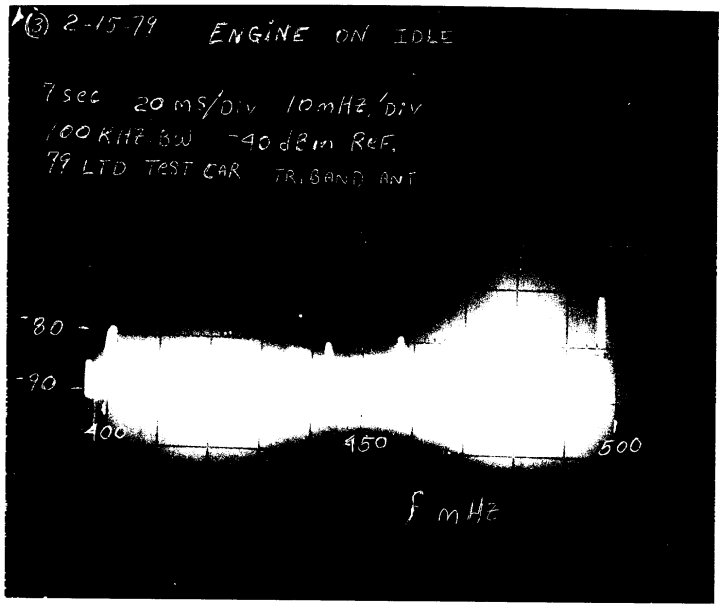

-10 dBm/division

10 MHz/division

(e) 400 to 500 MHz; Engine on.

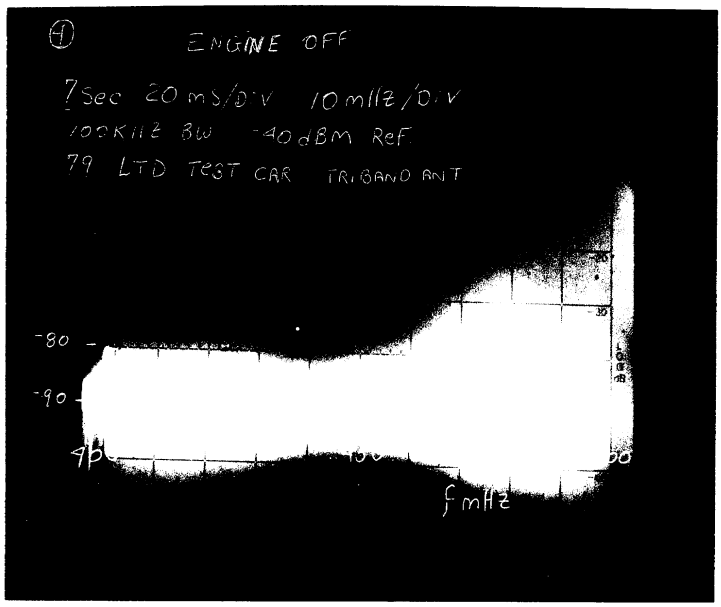

-10 dBm/division

10 MHz/division

(e') 400 to 500 MHz; Engine off.

Figure 7. (continued). Frequency domain signals obtained with Ford LTD.

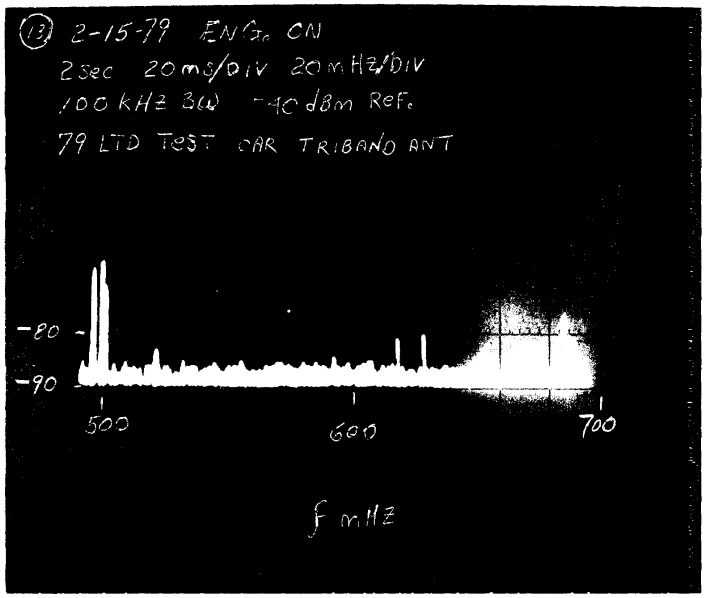

-10 dBm/division

20 MHz/division

(f) 500 to 700 MHz; Engine on.

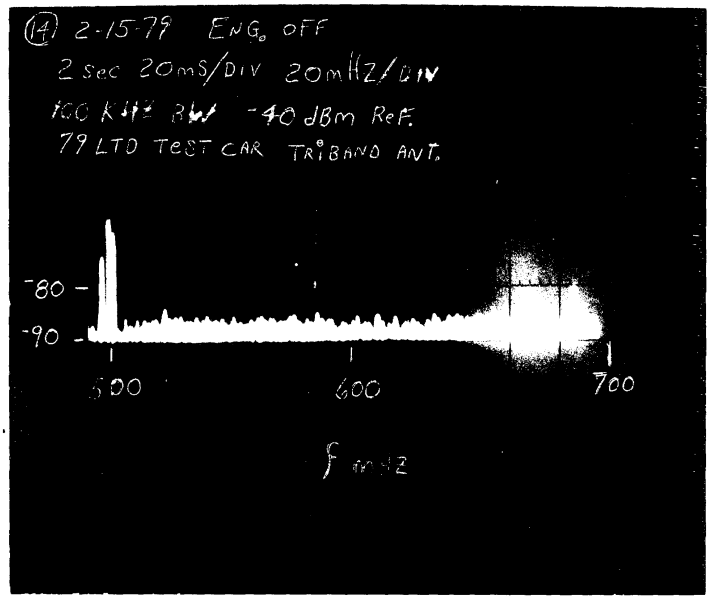

-10 dBm/division

20 MHz/division

(f') 500 to 700 MHz; Engine off.

Figure 7. (continued). Frequency domain signals obtained with Ford LTD.

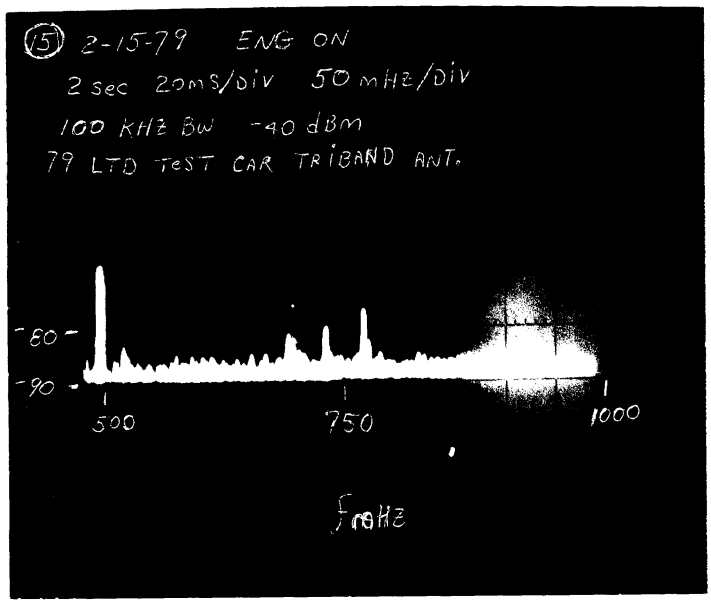

-10 dBm/division

50 MHz/division

(g) 500 to 1000 MHz; Engine on.

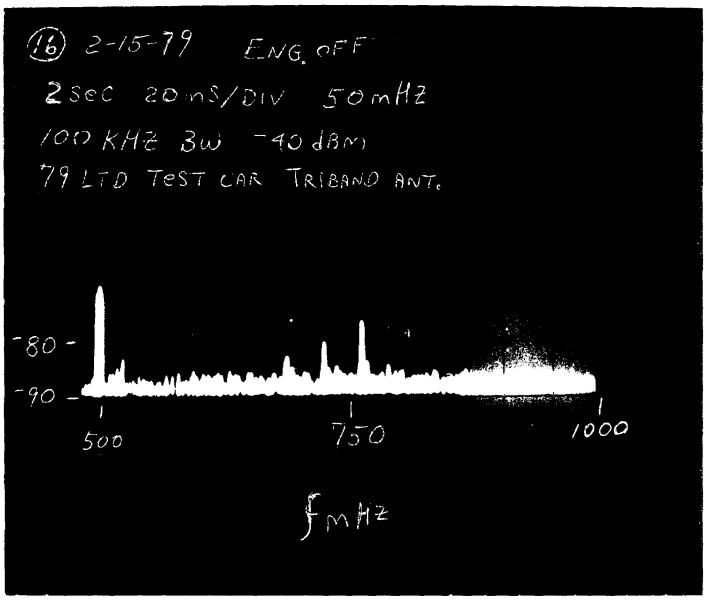

-10 dBm/division

50 MHz/division

(g') 500 to 1000 MHz; Engine off.

Figure 7. (continued). Frequency domain signals obtained with Ford LTD.

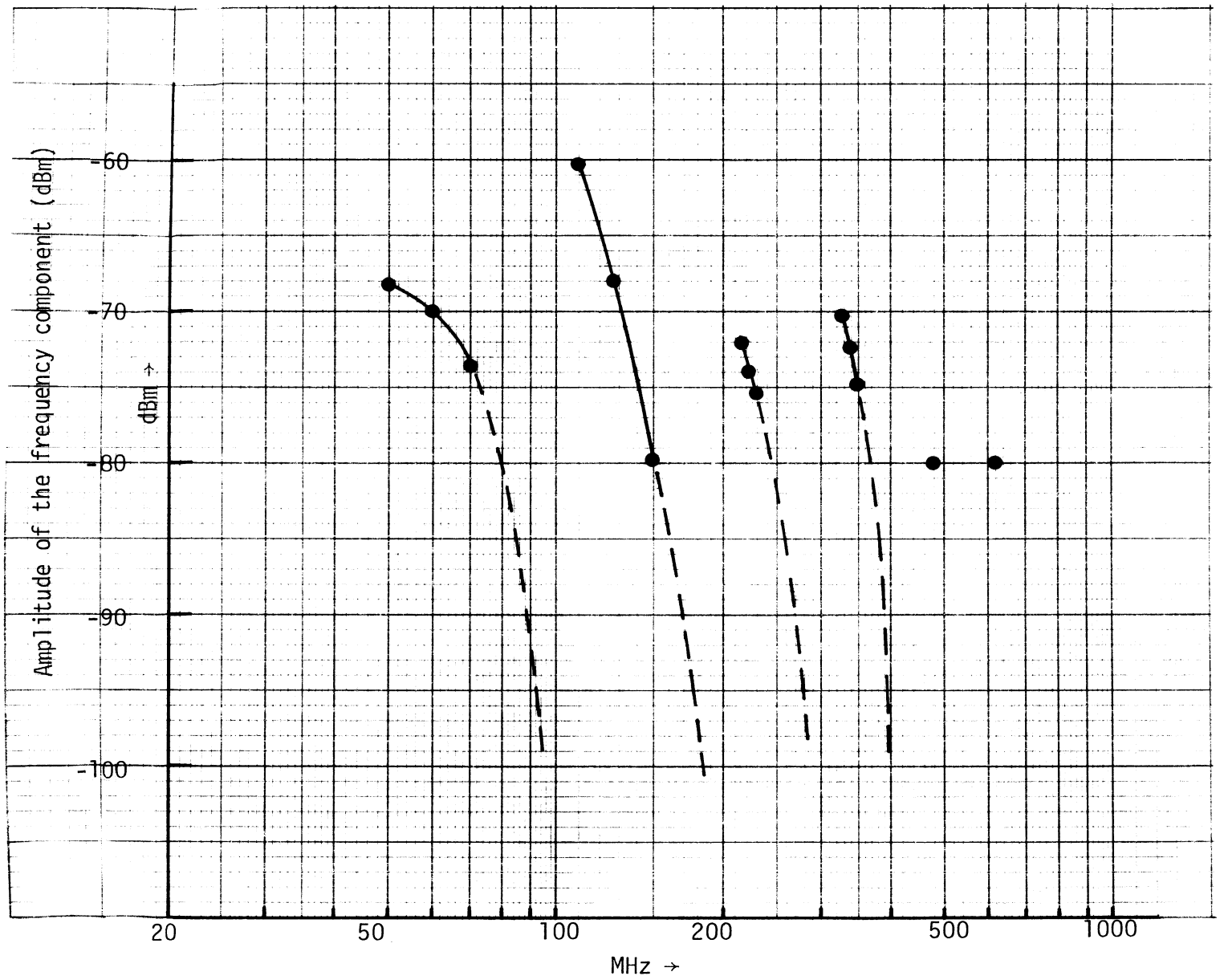

Figure 8. Amplitude distribution of the frequency components of the signal received with Ford LTD.

former effects would generally be variable in time and hard to characterize. Usually, the higher frequency components will suffer more space attenatuation. The antenna, being turned to 100 MHz attenuates the 70 MHz component more than the 100 MHz component and, consequently, the received signal shows a reduced amplitude at 70 MHz (Fig. 8) although the amplitude of this component in the original ignition pulse is higher.

2.4 Discussion

Automobile ignition system generated RFI signals at the entertainment antenna terminals of three test cars have been measured in the time and frequency domain. Generally, the received time domain signals are pulsed in nature, and signals originating from both the initial and subsequent ignition pulses have been observed. Very little resemblance has been observed between two or more received pulses.

It has been found that the front mounted antennas receive more RFI signals than the rear mounted antennas; windshield and front-mounted antennas on the same car receive RFI signals of the same order.

RFI signals received with Ford cars ranged typically between 20 - 40 mv; with the competitor car the received RFI signal was 400 mv.

III. SUSCEPTIBILITY OF AUTOMOBILE RADIOS TO IMPULSE NOISE

As mentioned in the introduction, the automobile ignition system generates short electromagnetic pulses or impulse noise signals which couple to the entertainment antenna of the automobile radio mainly by radiation mechanisms. In Chapter II it was found that the amplitude of such ignition generated noise signals, measured at the antenna terminals, was typically 400 mv for the competitor car and 20 - 40 mv for the two Ford cars. Under some conditions, these received signals may cause objectionable interference to the reception of desired signals by the radio system. The primary objectives of the investigation reported in the present chapter were to: (i) measure the performance characteristics of selected automotive radios receiving laboratory generated RF signals in the presence of laboratory generated impulse noise signals, and (ii) trace how the various stages of the radio respond to such injected noise signals. Although the measurements were carried out with controlled signals in a laboratory atmosphere, the results should be useful in estimating the vulnerability of the radios receiving outside broadcast signals in an actual automobile environment.

3.1 Test Set-Up

To eliminate the effects of external interference, all measurements were carried out inside a screened room. The block diagram shown in Fig. 9 gives the schematic arrangement of the equipment set up and used during the measurement.

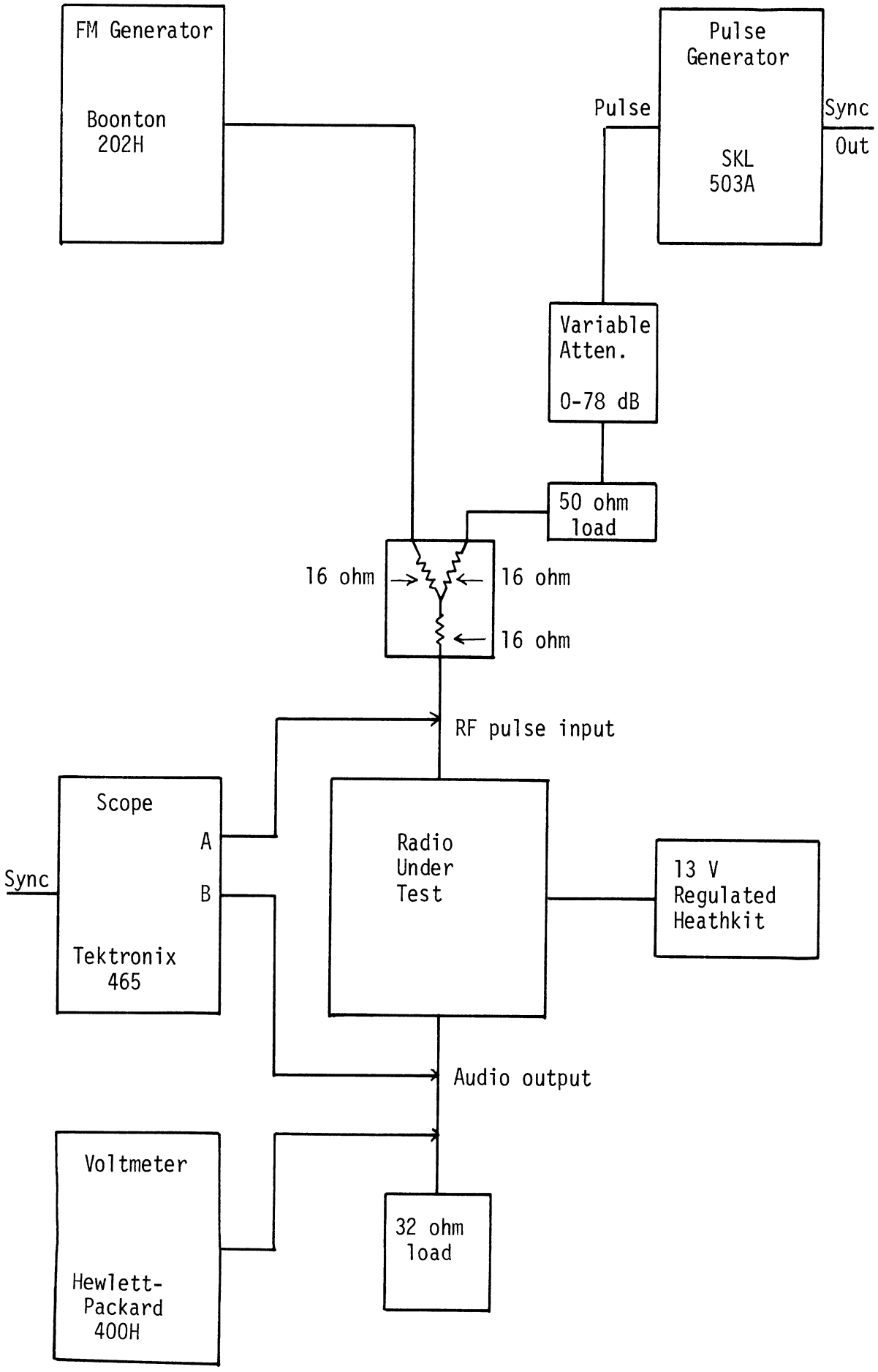

Figure 9. Block diagram showing the experimental arrangement used for susceptibility measurement.

As can be seen from Fig. 9, the three-port 50 to 100 ohm network made it possible to apply two independent signals, singly or together, to the input of the radio under test. The FM signal generator provided unmodulated or 1 kHz frequency modulated, variable amplitude, RF signals having variable frequencies within the FM broadcast band. The pulse generator, in combination with the variable attenuator, provided short pulses having variable amplitude, width and repetition rate. The dual trace oscilloscope monitored and measured the signals at the input and output terminals of the test radio, the latter signals being at audio frequencies. A voltmeter also measured the RMS voltage developed across a 3.2 ohm load simulating the impedance of a typical speaker. The radio under test obtained its power from a regulated power supply.

3.2 Standard Test Conditions

In order to obtain meaningful and consistent results throughout the investigation, the following standard test conditions, suggested by Fort Motor Co., were followed during the measurements:

(i) Set the test radio tone control to full clockwise (i.e., treble) position.

(ii) Turn the pulse modulation off.

(iii) Set FM modulation deviation to 25 kHz.

(iv) Set audio modulation frequency to 1 kHz.

(v) Turn the RF carrier frequency dial of the FM generator to the frequency of interest.

(vi) Set the input RF carrier amplitude level to 100,000 μv (i.e., 100 mv).

(vii) Turn the tuning frequency dial of the test radio to the frequency of step (v), and fine tune to obtain a clear 1 kHz sine wave on the oscilloscope at the radio output.

(viii) Adjust the volume control of the radio so that the RMS amplitude of the 1 kHz sine wave is 1.8 v (as measured across the 3.2 ohm resistor at the output of the receiver). Note: do not change the volume control setting during the remaining portion of the test.

(ix) Decrease the RF carrier amplitude level of the FM generator so that the RMS level of the 1 kHz sine wave, as measured acorss the 3.2 ohm resistor, is reduced to 1.6 v (i.e., -1 dB/W). Record the amplitude of the input RF carrier.

(x) Turn the pulse generator on.

(xi) Set the pulse width and repetition rate to desired values.

(xii) Adjust the amplitude of the input pulse until a signal just above the signal obtained in (ix) is observed on the scope at the output.

(xiii) Measure and record the amplitude of the input pulse.

(xiv) Repeat steps (i) - (xiii) for each RF frequency of interest.

(xv) Repeat steps (i) - (xiv) for each pulse width of interest.

(xvi) Repeat steps (i) - (xv) for each repetition rate of interest.

3.3 Radio Response to Short Pulses

For a given threshold of noise at the output of the test radio, the required amplitude of the input pulse as a function of the tuning frequency of the radio was obtained for a number of typical automobile radios. The frequency of the input RF carrier signal (and/or the tuning frequency) was varied over the entire band of FM broadcast frequencies, and results were obtained with and without modulation of the RF carrier.

3.3.1 AM-FM Radio: F2

Description of Results

This section discusses the results obtained with an AM-FM-MPX test radio referred to as F2. Figure 10 shows the results obtained with the test radio F2 for an input pulse having a width τ = 10 ns (as read from the pulse generator) and repetition rate of 100 Hz. The actual width of the pulse, as measured with the oscilloscope, was τ = 9.5 ns. The general nature of variations of the results shown in Fig. 10 are found to be similar with and without modulation of the input RF carrier signal. For input carrier frequency $f_c \lesssim$ 100 MHz the two results are almost identical; however, for $f_c >$ 100 MHz the required amplitude

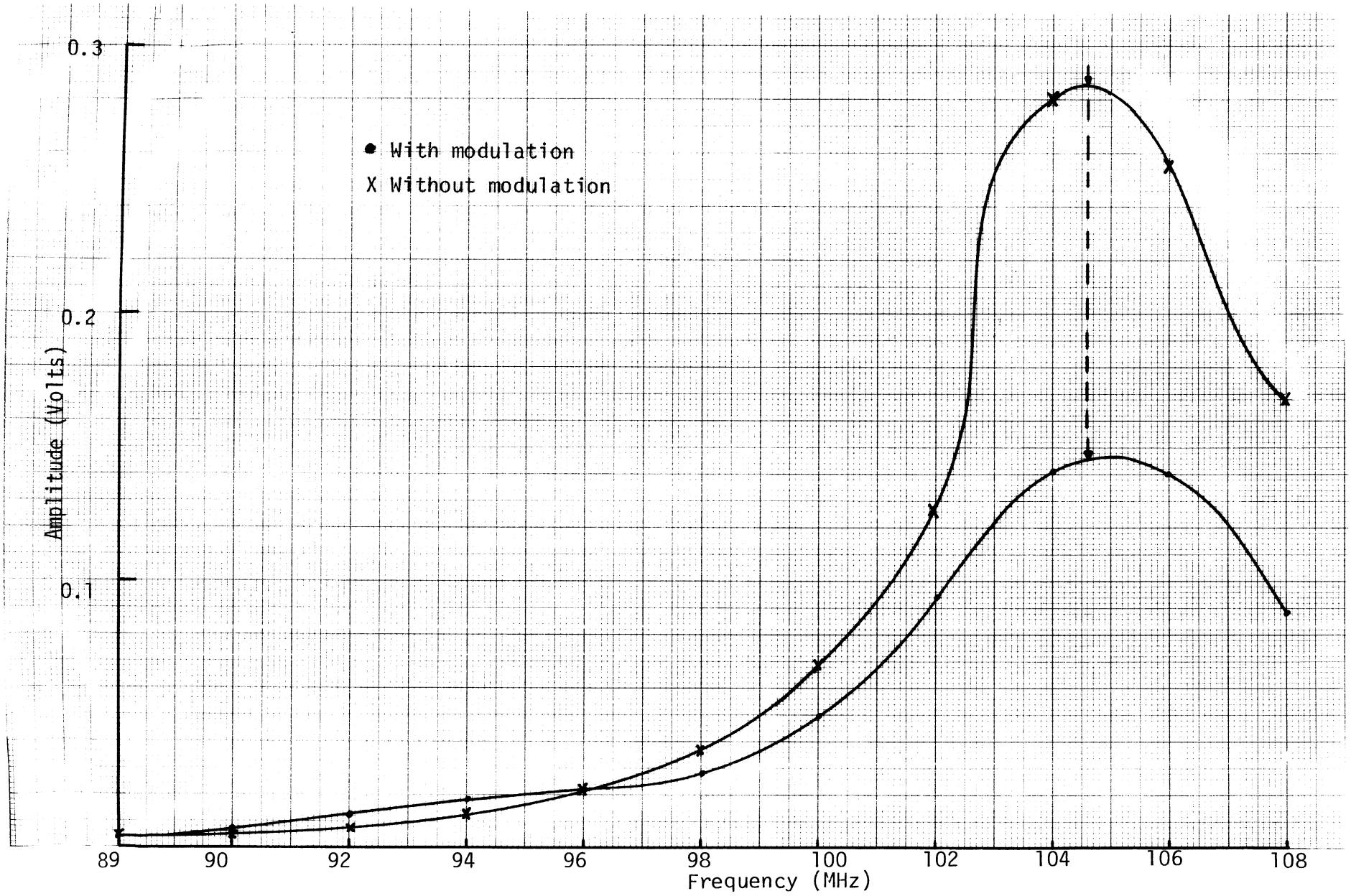

Figure 10. Amplitude of the input pulse vs. radio tuning frequency required for threshold noise at the output. Pulse width = 9.5 ns, repetition rate = 100 Hz, Test Radio: AM-FM-F2.

of the input pulses are found to be significantly larger with unmodulated RF carrier. In both cases, the required pulse amplitude, at first increases very slowly with f_c up to $f_c \simeq 100$ MHz, and then for $f_c \gtrsim 100$ MHz, rapidly assumes a maximum value (at $f_c \simeq 104$ to 106 MHz); finally, it decreases rapidly with f_c near the end of the band of frequencies used. However, the results of Fig. 10 do not necessarily mean that, for $f_c > 100$ MHz, the test radio is less vulnerable to interference caused by the 10 ns input pulse, and also that the absence of modulation in the RF carrier makes the pulse less objectionable. As will be discussed later, this phenomenon is associated with the amplitude distribution of the frequency spectrum of the input pulse, rather than the characteristics response of the radio itself. Therefore, it is argued that the radio responses to impulsive noise are similar for modulated and unmodulated RF input signals; the larger values obtained with unmodulated RF carrier, as shown in Fig. 10, merely indicate that it was more difficult to judge and qualify the audio output noise and, therefore, required longer amplitude input pulses.

Similar sets of results obtained with input pulses with variable widths, and with unmodulated RF carrier input signals, are shown in Fig. 11. Observe the peaks at 94.3 MHz and 104 ns for $\tau = 10.6$ ns and 9.5 ns, respectively; also note the absence of peaks for $\tau < 9.5$ and $\tau > 10.6$ ns.

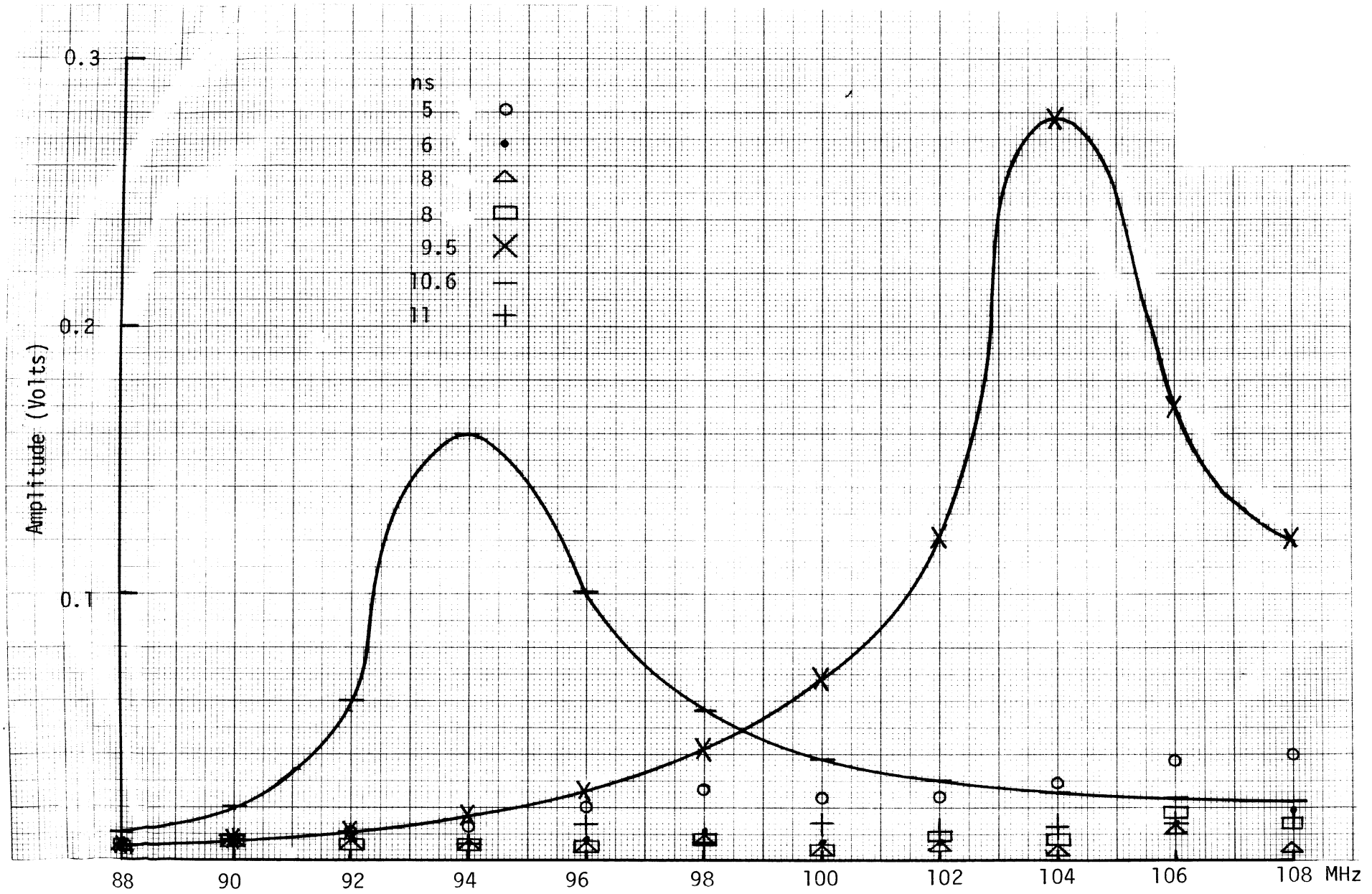

Figure 11. Amplitude of the input pulse vs. radio tuning frequency required for threshold noise at the output. Pulse width variable, repetition rate = 100 Hz.

The results also indicate that the radio responds almost the same way to all the pulses used, except for those with τ = 9.5 and 10.6 ns. Figure 12 shows similar results obtained with a wider input pulse having τ = 67 ns; note the two peaks occurring at approximately 90 and 105 MHz, respectively.

Analysis of Results

The behavior of the results presented above may be understood better by studying the frequency spectrum of the input pulses. Let the input signal consisting of a rectangular pulse of width τ and amplitude A repeat every T seconds. Such a train of pulses may be represented as a function of time by

$$f(t) = \begin{cases} A & \text{for } -\frac{\tau}{2} < t < \frac{\tau}{2} \\ \\ 0 & \text{for } \frac{\tau}{2} < t < T - \frac{\tau}{2} \end{cases} . \qquad (1)$$

It can be shown [5] that f(t) given by (1) has the following Fourier series representation:

$$f(t) = \frac{A}{T} \sum_{n=-\infty}^{\infty} \frac{\sin(n\omega_0\tau/2)}{(n\omega_0\tau/2)} e^{jn\omega_0 t} , \qquad (2)$$

where $\omega_0 = 2\pi/T$ is the fundamental radian frequency and is related to the fundamental frequency f_0 by $\omega_0 = 2\pi f_0$.

It is evident from (2) that the frequency spectrum of the input signal, given by (1), is a discrete function which exists only at $\omega = 0, \pm\omega_0, \pm 2\omega_0, \ldots$etc., and has amplitudes $A\tau/T$, $A\tau/T[\sin(\omega_0\tau/2)/\omega_0\tau/2]$, $A/T[\sin(\omega_0\tau)/(\omega_0\tau)]$,...etc., respectively. In the present case $\tau/T << 1$,

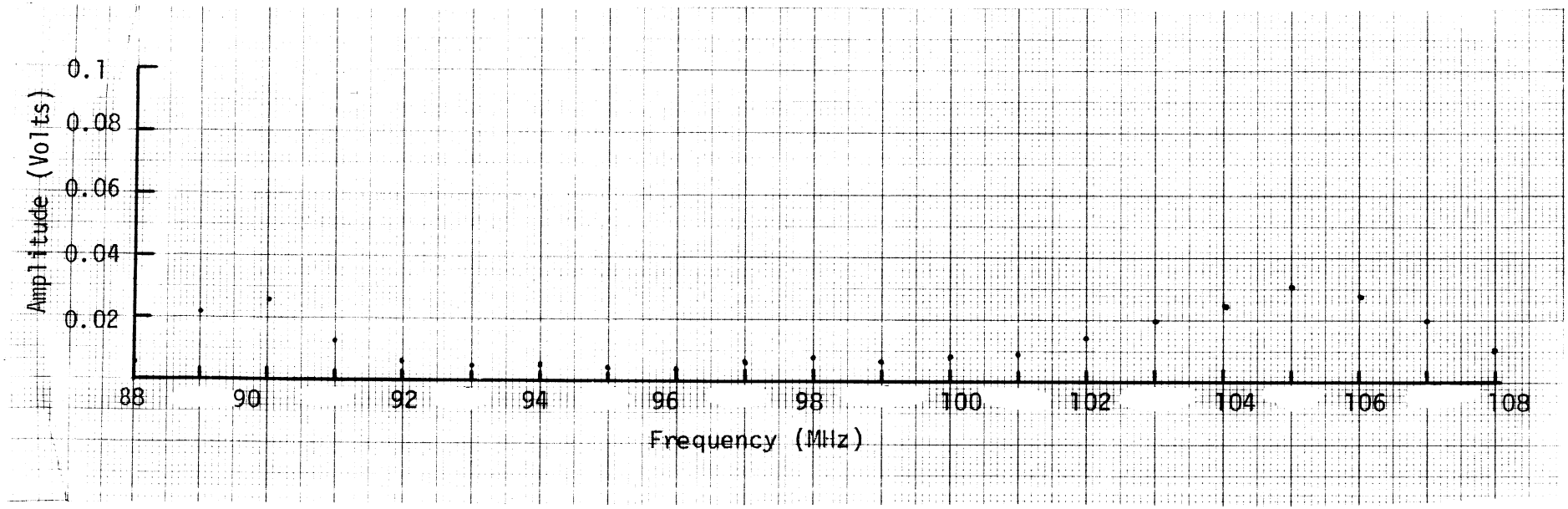

Figure 12. Amplitude of the input pulse vs. radio tuning frequency required for threshold noise at the output. Pulse width = 67 ns, Repetition rate = 100 Hz, Test Radio: AM-FM-F2.

and we can use the following continuous function for the frequency spectrum of the input signal:

$$F(\omega) = \frac{A\tau}{T} \frac{\sin(\omega\tau/2)}{(\omega\tau/2)} , \qquad (3)$$

where $\omega = 2\pi f$, now refers to a continuously variable frequency of the component having an amplitude $|F(\omega)|$. The variation of $\sin(\omega\tau/2)/(\omega\tau/2)$ as a function of $\omega\tau/2$ is shown in Fig. 13 from which amplitude $|F(\omega)|$ of a frequency component of angular frequency ω may be obtained for a given periodic train of pulses provided, $\tau/T << 1$.

Note that (3) and Fig. 13 indicate that $F(\omega) = 0$, whenever $\omega\tau/2 = m\pi$ where m = 1,2,...etc. This implies that the following frequency components will be absent from the frequency spectrum of a pulse of width T.

$$f_m = \frac{m}{\tau} , \quad m = 1,2,.... \qquad (4)$$

Table 2 shows some selected frequency components, as obtained by using (4), which are absent from the frequency spectrum of a pulse having

Table 2

Missing Frequencies in the Frequency Spectrum

Pulse Width τ(ns)	Missing Frequency f(MHz)
5	200
6	167
7	143
8	125
9	111
10	100
11	91
12	83
67	89.4, 104.3

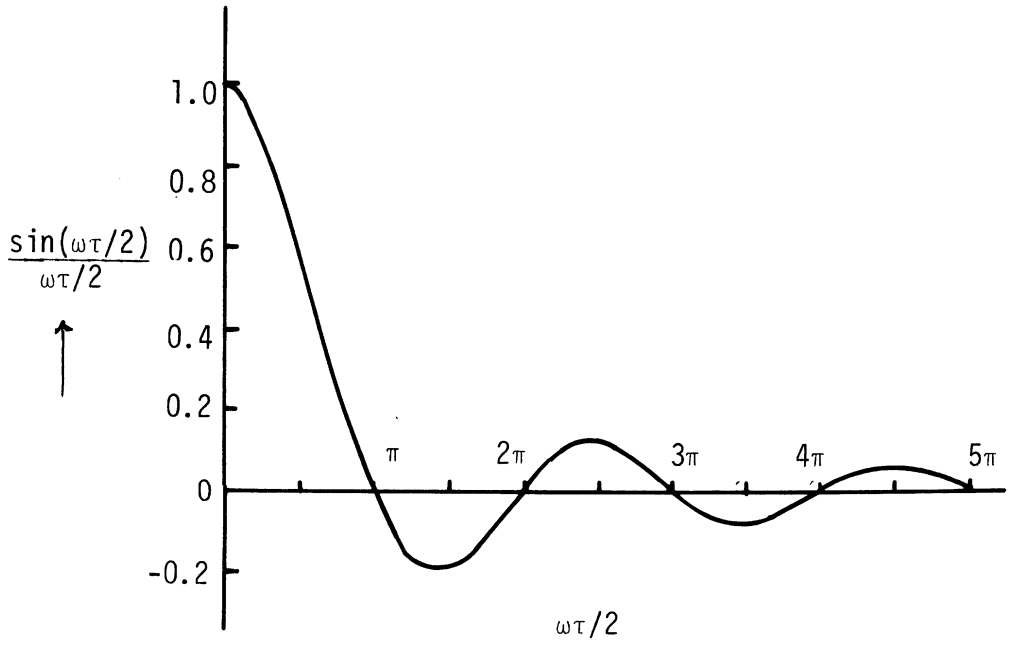

Figure 13. $\sin(\omega\tau/2)/(\omega\tau/2)$ vs $(\omega\tau/2)$ used for obtaining the amplitude of various frequency components.

various widths τ. Note that the missing frequencies shown in Table 2, for τ = 5 to 12 ns, have been obtained with m = 1; for τ = 67 ns, the two missing frequencies have been obtained with m = 6 and 7, and are within the FM broadcast band of frequencies.

It is now simple to explain the behavior of the results shown in Figs. 10 and 11. For example, the two peaks in Fig. 10 occur at approximately the theoretical first missing frequency f_1 = 105.3 MHz for the pulse having τ = 9.5 ns. Similarly, in Fig. 11 the two peaks in the results for τ = 9.5 and 10.6 ns occur approximately at the corresponding theoretical first missing frequencies 105.3 and 94.3 MHz, respectively. The results shown in Fig. 11 for other values of τ do not have any peaks because the missing components of the frequency spectrum of the input pulse were outside the FM broadcast band (see Table 2). The two peaks in Fig. 12 occur at frequencies very near the theoretical frequencies for τ = 67 ns as given in Table 2.

It is now argued that the occurrence of maxima at certain frequencies, as shown in Figs. 10 through 12, is due to the absence (or reduced amplitudes of those frequency components from the spectrum of the input pulses. Consequently, when the radio was tuned near those frequencies increased pulse amplitudes were required to obtain the same amount of threshold noise at the output. As mentioned earlier, this behavior of the results are determined by the input pulses used, and is not a characteristic property of the test radio.

3.3.2 Results for Other Radios. The pulse amplitudes required to obtain a given threshold of noise at the output were measured for a number of typical automotive radios, and for given pulse widths and

repetition rates. In all, eleven test radios were used; they are identified as shown in Table 3.

Table 3

Identification of Test Radios

Type	Identification	Number of Radios
AM-FM	F1, F2, F3	3
AM-FM-MPX (Multiplex)	M1, M2, M3	3
AM-FM-MPX-Tape (8-Track)	T1	1
AM-FM-MPX-Cassette	C1, C2	2
All Electronic	E1, E2	2

Figure 14 shows the results obtained with the test radios, identified in Table 3 and using input signals consisting of a modulated 100 MHz RF carrier and 9.7 ns wide short pulser repeating at 100 Hz. All test radios were adjusted as per test conditions, given earlier. The general behavior of the results for all the test radios appear to be similar; all the results assume maximum values at a frequency near 103 MHz ($\simeq 1/\tau$, with τ = 9.7 ns) which is the missing frequency component in the spectrum of a 9.7 ns pulse.

The input pulse amplitudes required to obtain the threshold noise output, with input pulses having variable pulse widths and repetition rates are shown in Table 4 for the eleven test radios. In all cases the radio was tuned to 100 MHz RF input signal which was 1 kHz frequency modulated with 22.5 kHz frequency deviation; otherwise, the test conditions outlined in Section 3.2 were followed. The results shown in Table 4 indicate that the pulse repetition rates have little effect on the required amplitudes

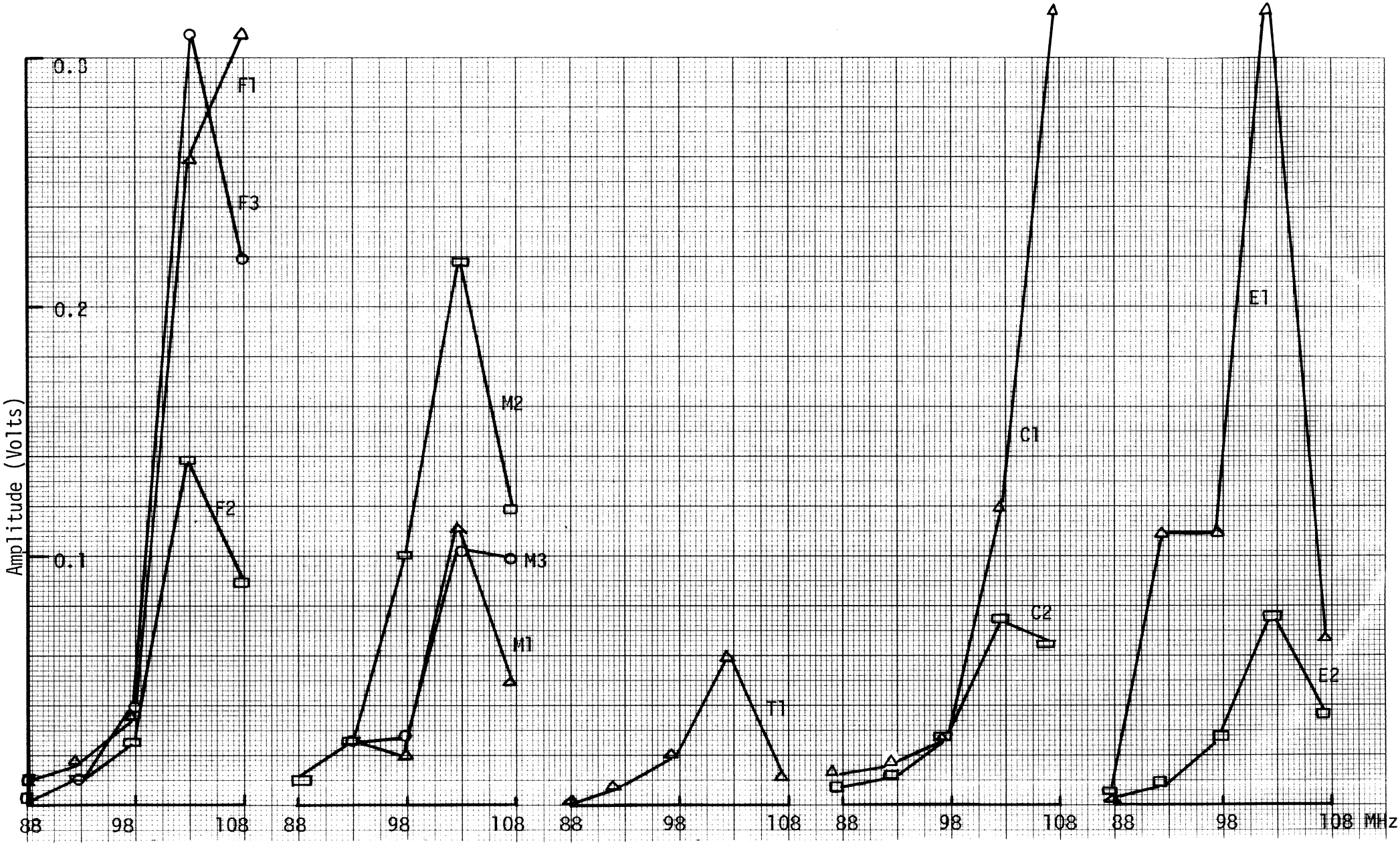

Figure 14 Amplitude of the input pulse vs. radio tuning frequency required for threshold output noise for various test ratios. Pulse width = 9.7 ns, repetition rate = 100 Hz.

Table 4

Pulse Response of Test Radios

Radio	Pulse Rep. Rate (Hz)	Input Pulse Width (ns)	Input Pulse Amplitude (V)
F1	150	10	0.198
	50	10	0.314
	150	100	0.043
	50	100	0.048
F2	150	10	0.140
	50	10	0.198
	150	100	0.027
	50	100	0.030
M1	150	10	0.079
	50	10	0.089
	150	100	0.015
	50	100	0.019
M2	150	10	0.056
	50	10	0.089
	150	100	0.012
	50	100	0.015
T1	150	10	0.056
	50	10	0.079
	150	100	0.011
	50	100	0.015
C1	150	10	0.044
	50	10	0.079
	150	100	0.017
	50	100	0.017
C2	150	10	01070
	50	10	0.079
	150	100	0.015
	50	100	0.017
E1	150	10	0.035
	50	10	0.050
	150	100	0.009
	50	100	0.004
E2	150	10	0.050
	50	10	0.070
	150	100	0.012
	50	100	0.015

of the input pulses; with 10 ns pinpoint pulses, all radios require increased pulse amplitudes for observable audio noise at the output. This is consistent with the theory that a 10 ns pulse has a missing frequency component at 100 MHz and consequently the radios being tuned near 100 MHz required stronger input pulses for observable noise.

3.4 Short Pulse Response of Various Stages of a Test Radio

This section describes the results of an investigation conducted to study the response of various stages of a test radio to input signals containing a train of repetitive short pulses. An AM-FM-MPX type of test radio, designated by M1, was used during this set of measurements.

3.4.1 Test Set-Up. The basic experimental set-up shown in Fig. 9 was used for the input-output measurements. Figure 15 gives a block diagram outlining the method employed to examine the signals at selected test points (shown as TP-A, TP-B etc.) located at various stages of the test radio. The test points (TP) were carefully selected so that the placement of the test probe at these points did not load the circuit and thereby influence the radio performance. A test point was selected if, with a given input signal, the audio output monitored by the oscilloscope at the output end did not change with and without the test probe placed at that point. Five test points, TP-A,B,...,E, selected in this manner are shown in Fig. 15. The RF and short pulse signals, as required, were applied to the input of the test radio in a manner shown in Fig. 9.

3.4.2 Tracing of the Input Pulse Signal Through the Radio. The test radio was initially adjusted to standard test conditions, and the input RF carrier signal was then switched off and a nominal 10 ns pulse

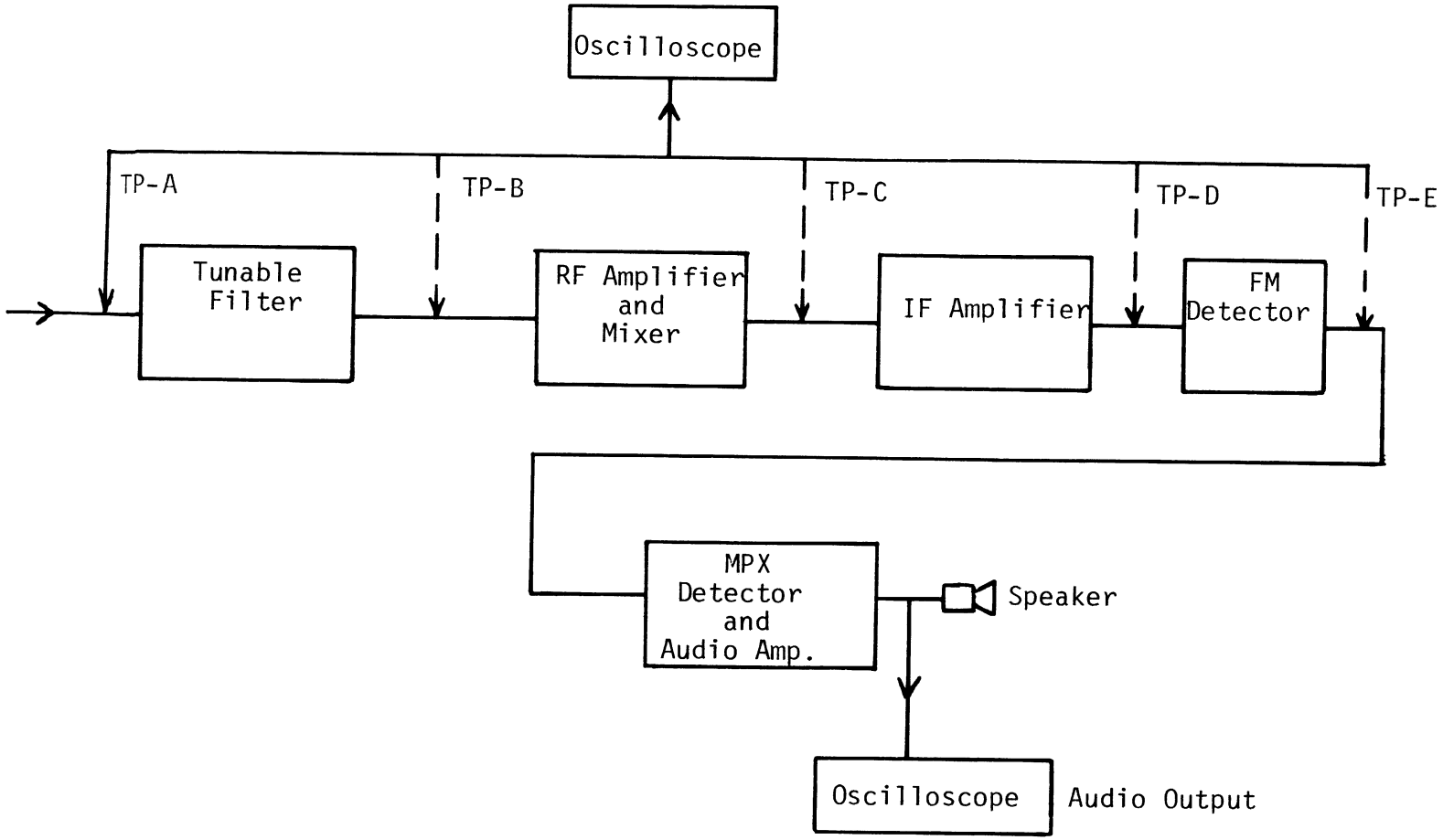

Figure 15. Diagram showing the various test points selected in a test radio.

signal repeating at 100 Hz was applied to the input. The upper and lower traces in Fig. 16 show the probe output signals at TP-A and TP-B, respectively. Test point A being located at the input, the TPA-signal in Fig. 16 indicates the actual signal applied at the input of the test radio; the second hump in the observed signal is attributed to ringing in the 3-port, 50 to 100 ohm impedance transformer (as shown in Fig. 9). At test point B the signal has passed through the tunable filter whose response is controlled by the setting of the RF tuning dial of the test radio. Hence, ideally a single frequency signal should be present at TP-B--this is evident from the TP-B signal, in Fig. 16, which contains predominantly a single frequency component. Table 5 shows the radio tuning dial setting and the corresponding dominant frequency of the TP-B signal as obtained from the oscilloscope reading for an input pulse of 25 ns width. The results shown in Table 5 indicate that the tunable filter passes those frequency components of the input pulse to which the radio is tuned, as it should.

Table 5

Observed Frequency of the Signal vs. Radio Tuning Dial Setting

Radio Tuning Dial Setting (MHz)	Oscilloscope Reading (0.05 μs/div)(cycles/3 div)	Frequency from Oscilloscope Reading (MHz)
108	16 1/2	110
98	15	100
88	13 1/2	90

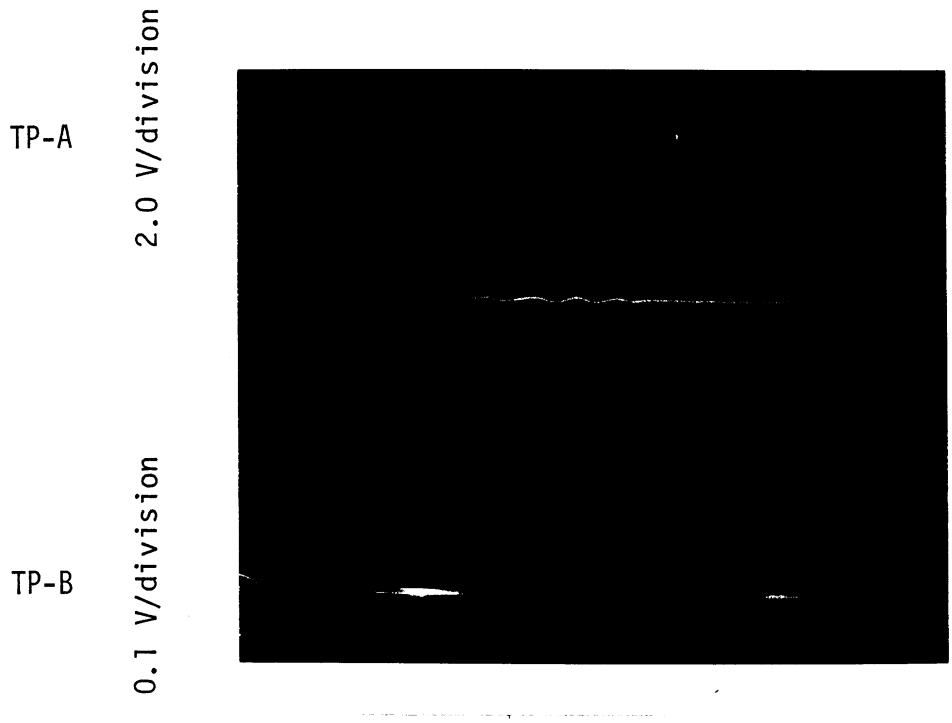

Figure 16. Signals at test points A and B.

For a given input pulse signal at A, it is of interest to know the amplitude of the signal at B as a function of the setting of the radio tuning dial, i.e., frequency of the signal at B. With a 9.5 ns wide input pulse the measured signal amplitude at B at various frequencies are shown in Table 6.

Table 6

Signal Amplitude at B as a Function of Frequency

(τ = 9.5 ns, repetition rate = 100 Hz, input pulse amplitude = 2 volts)

Radio Dial Frequency (MHz)	Signal Amplitude at B (volts)
88	0.12
90	0.12
92	0.11
94	0.10
96	0.08
98	0.07
100	0.05
102	0.04
104	0.02
106	0.03
108	0.04

The quantity $(1/V) \times 5.4 \times 10^{-3}$ (with V, as given in Table 6 and 5.4×10^{-3}, a scale factor), as a function of frequency is shown in Fig. 17. Earlier, in Fig. 10 we showed the input signal voltage required for a given output

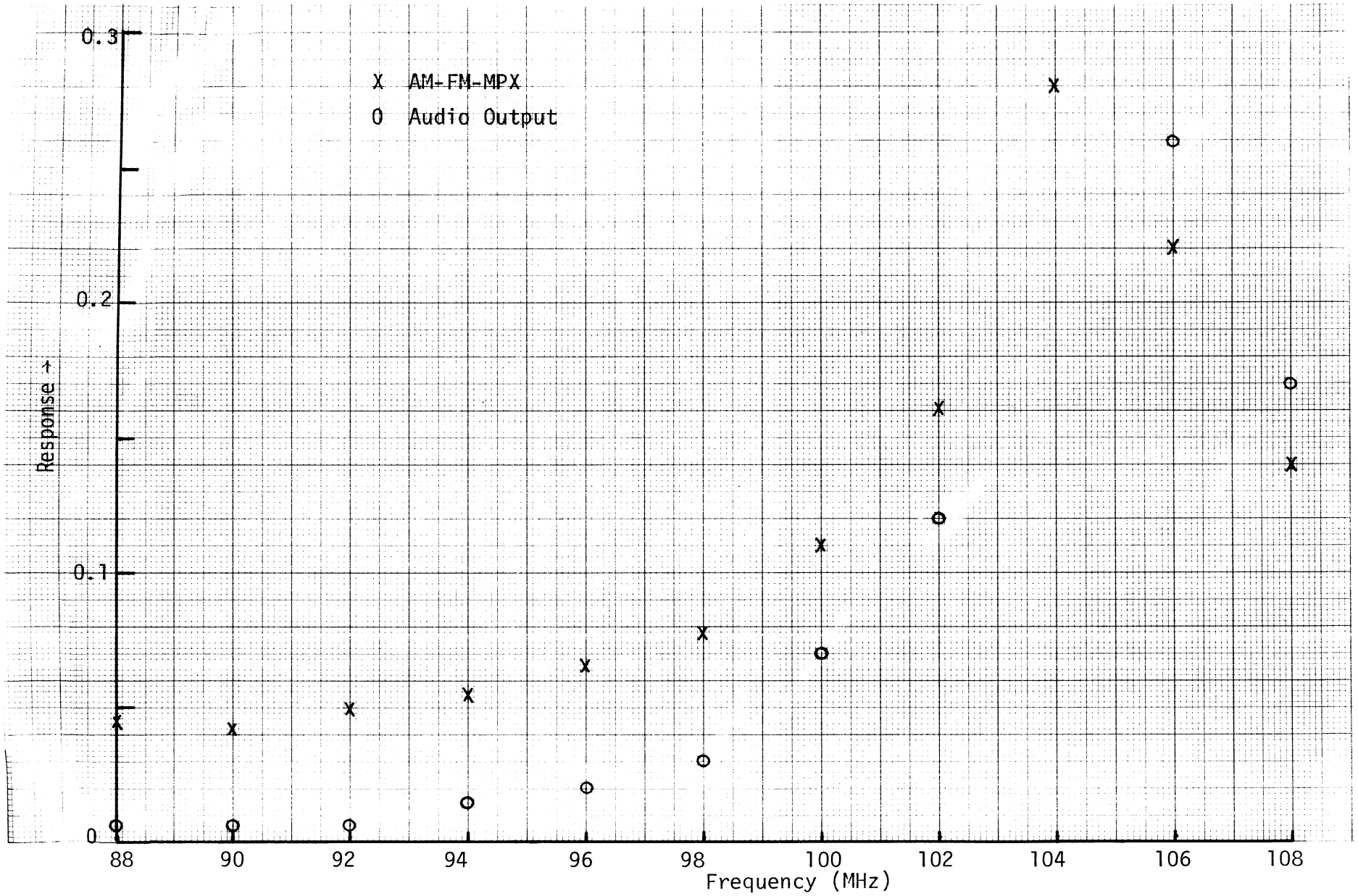

Figure 17. Reciprocal of normalized signal voltage at TP-B and the audio output vs. radio tuning frequency.

noise, for different frequencies. The top curve (without modulation) in Fig. 10 is shown also in Fig. 17 and it is found that the two results behave similarly; this is due to the tuned filter characteristics.

The signals obtained at various other test points with 9.5 ns input short pulse and the radio dial tuned to 90 MHz, are shown in Figs. 18 through 21. Test point C is located after the RF amplifier and mixer; hence, any signal appearing at C should be at the IF frequency of 10.7 MHz. The top traces of Figs. 18 and 19 show the signal at TP-C. The two lower traces of Figs. 19 and 20 represent the signal at test point D which is an amplified version of the signal at C. The upper traces of Figs. 20 and 21 represent the signal at test point E located after the FM demodulator; they clearly show that the initial input pulse has been stretched in time after passing through the various stages of the radio. The lower trace in Fig. 21 shows the observed audio output signal due to the input short pulse; note that shaped audio output signal waveform is due to the fact that the audio amplifier cannot react to the sharp rise and fall of the TPE signal shown in Fig. 21.

3.4.3 Response of the Radio to RF Carrier and Short Pulse Inputs. This set of measurements was carried out with an input signal consisting of a frequency modulated RF carrier plus repetitive short pulse signals. The upper and lower traces in Fig. 22 shows the signals at test points E and D, respectively, obtained with an input short pulse signal (no RF carrier signal input); these results are similar to those given earlier. With a combined RF carrier and short pulse input signals, the observed signals at various test points under various conditions are shown in Figs. 23 through 27.

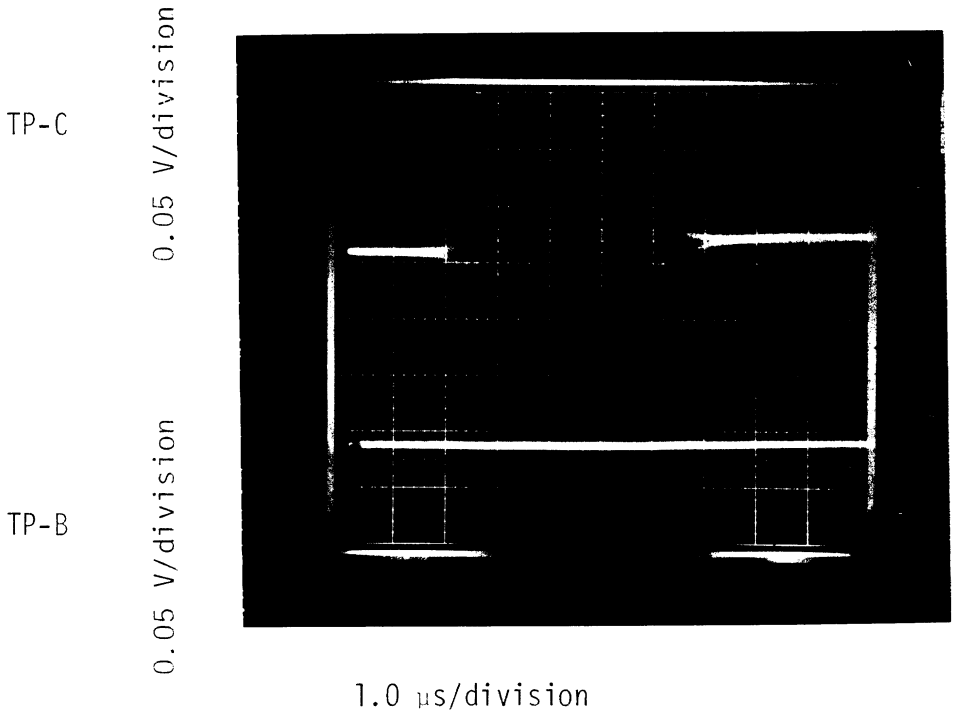

Figure 18. Signals at test points C and B.

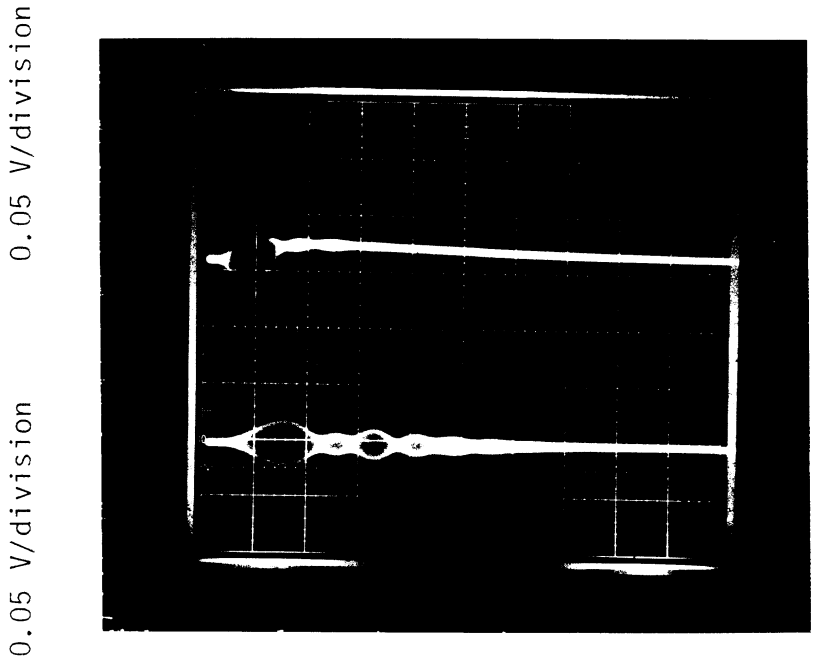

Figure 19. Signals at test points C and D.

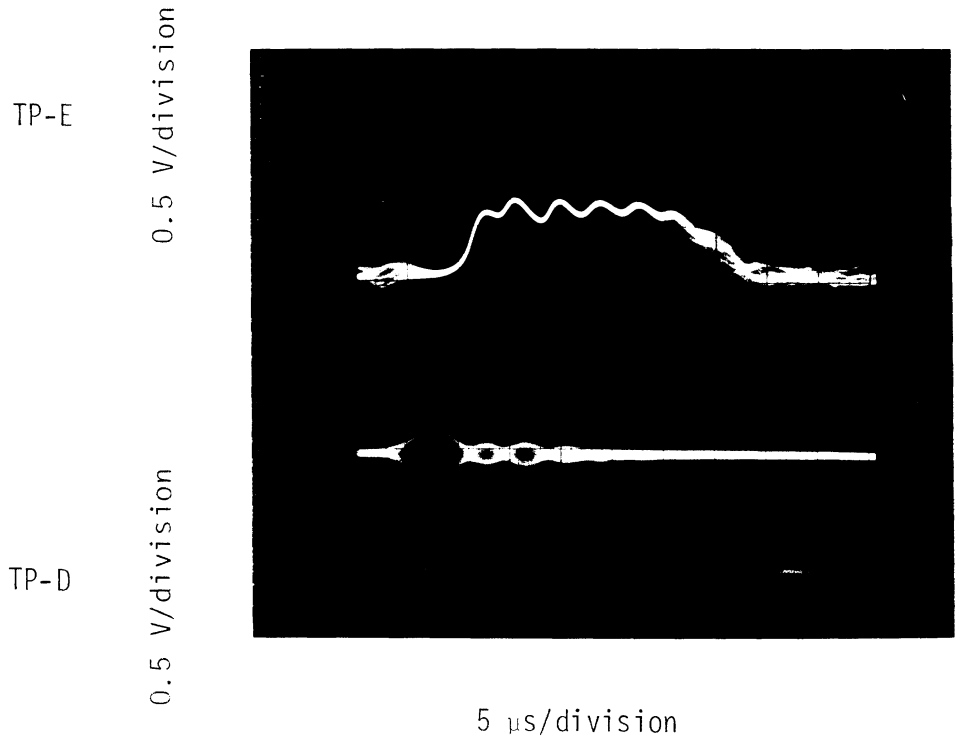

Figure 20. Signals at test points E and D.

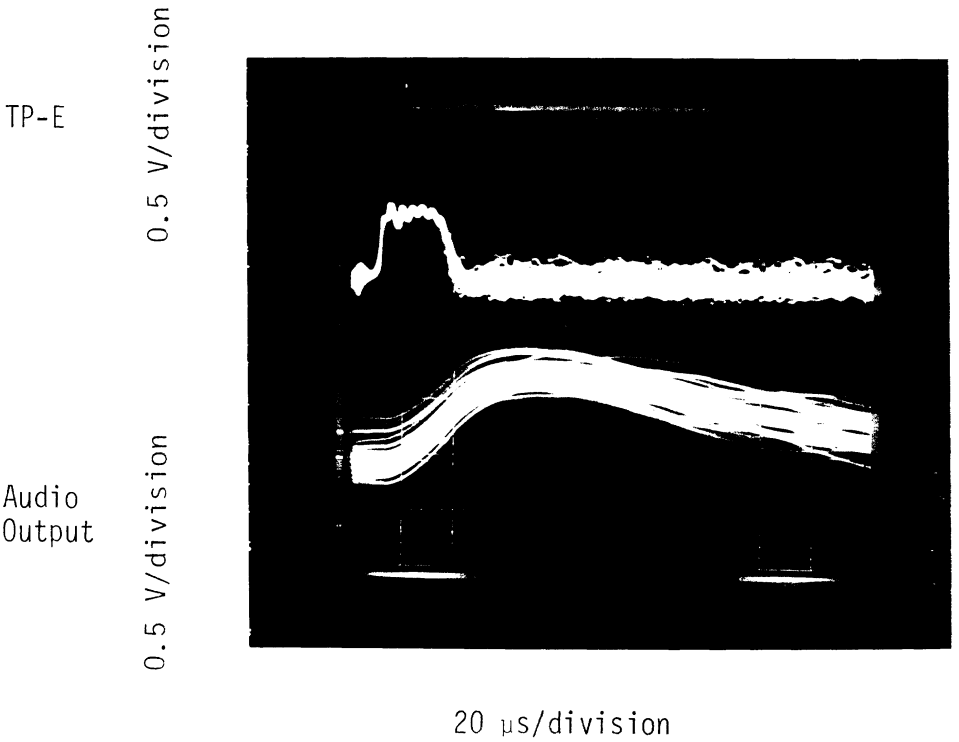

Figure 21. Signals at test point E and at the audio output terminal.

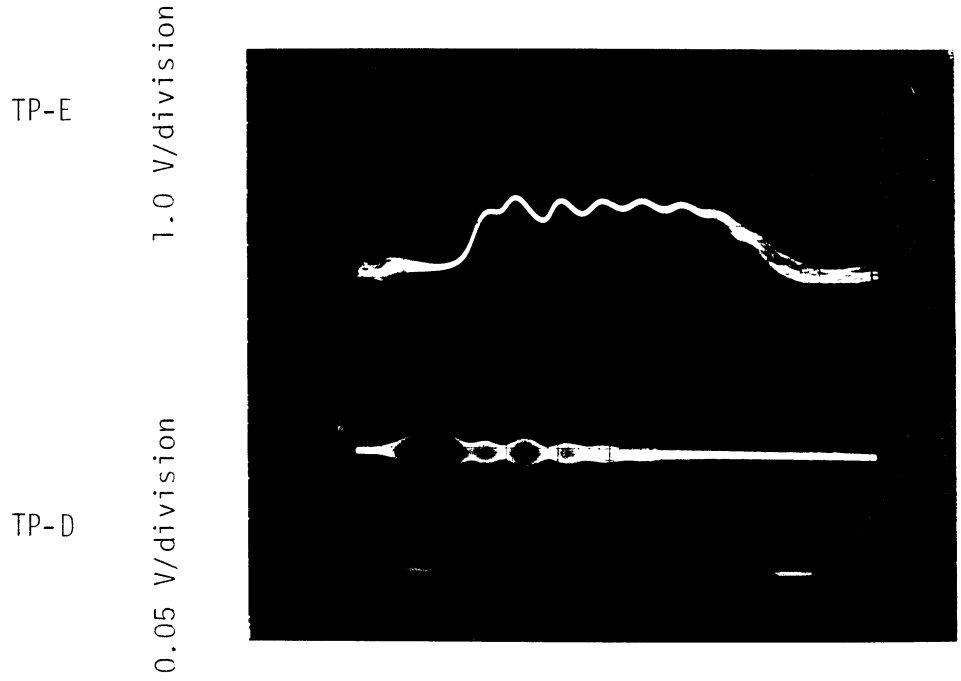

Figure 22. Signals at test points E and D with short pulse input and no RF carrier.

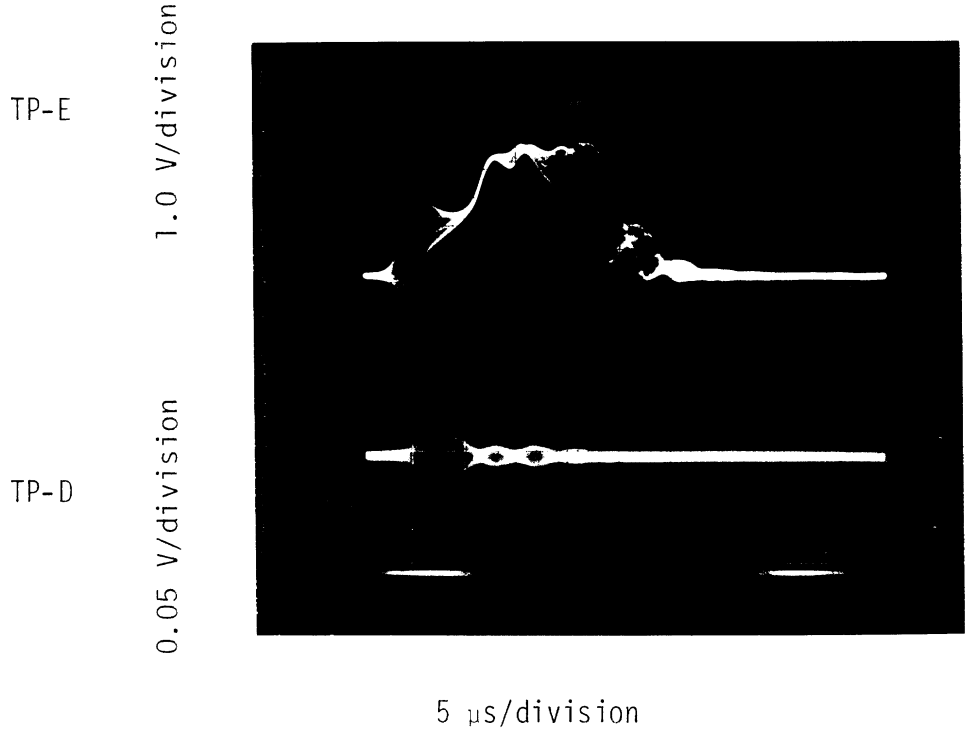

Figure 23. Signals at test points E and D with short pulse plus RF carrier input. RF carrier ampliutde = 100 μV.

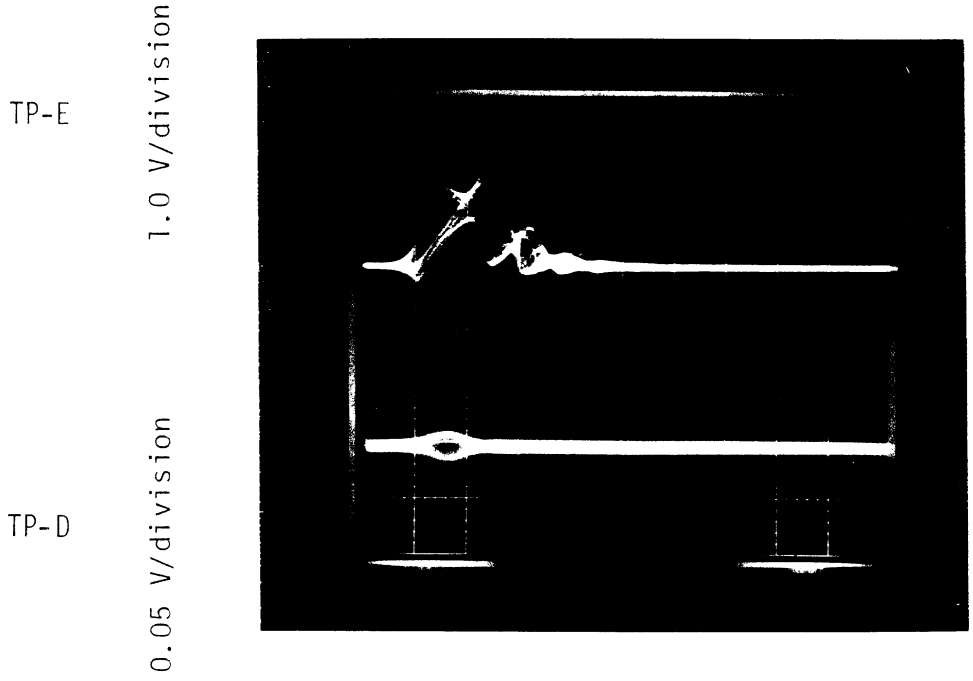

Figure 24. Signals at test points E and D with short pulse plus RF carrier input. RF carrier amplitude = 1000 μV.

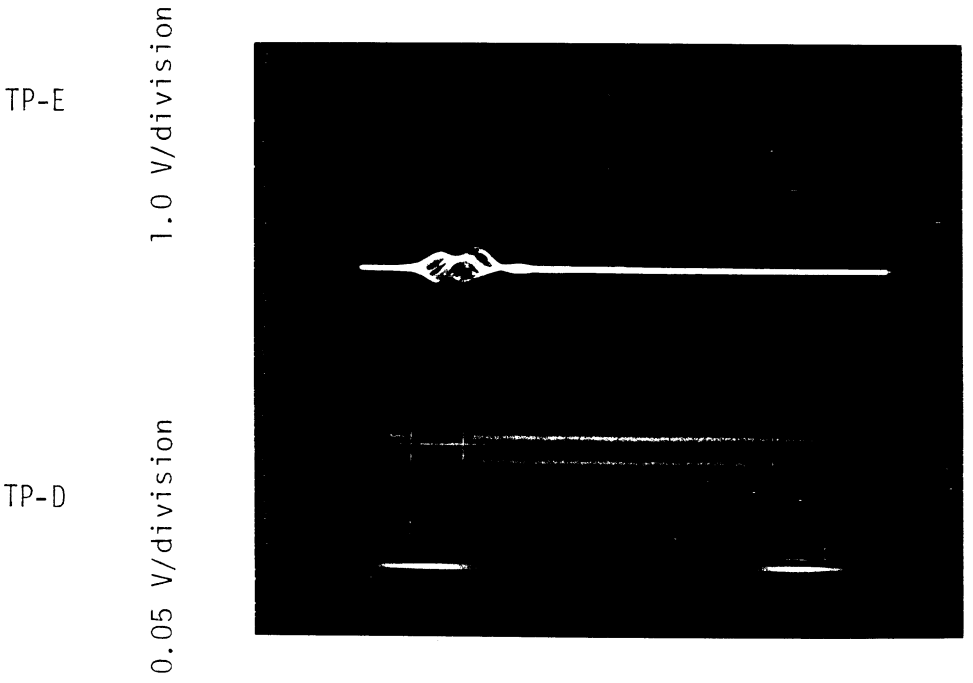

Figure 25. Signals at test points E and D with short pulse plus RF carrier input. RF carrier amplitude = 5000 μV.

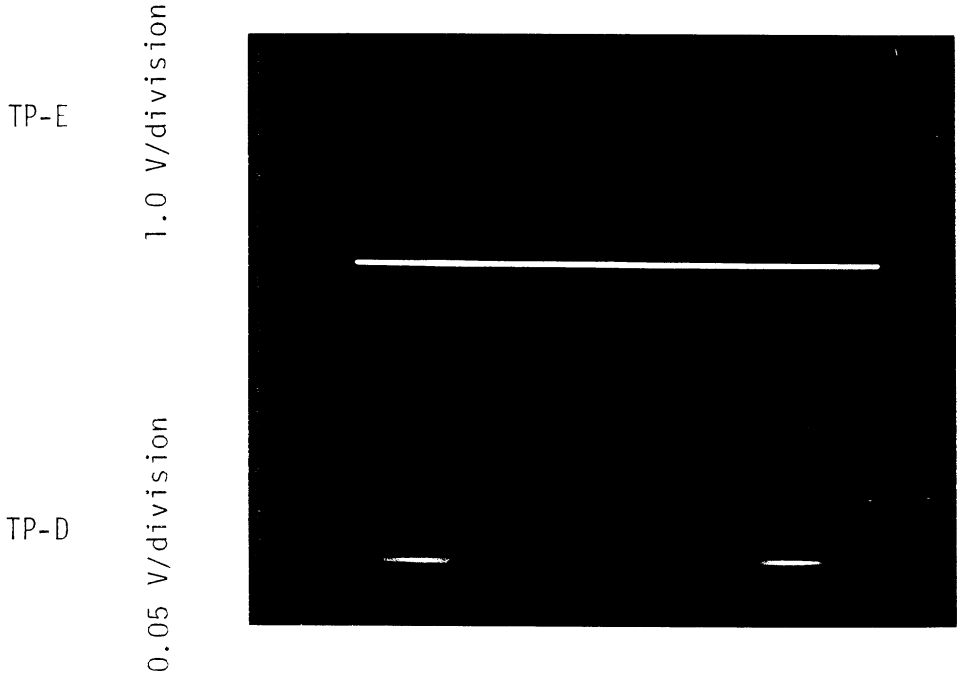

Figure 26. Signals at test points E and D with short pulse plus RF carrier input. RF carrier amplitude = 50,000 μV.

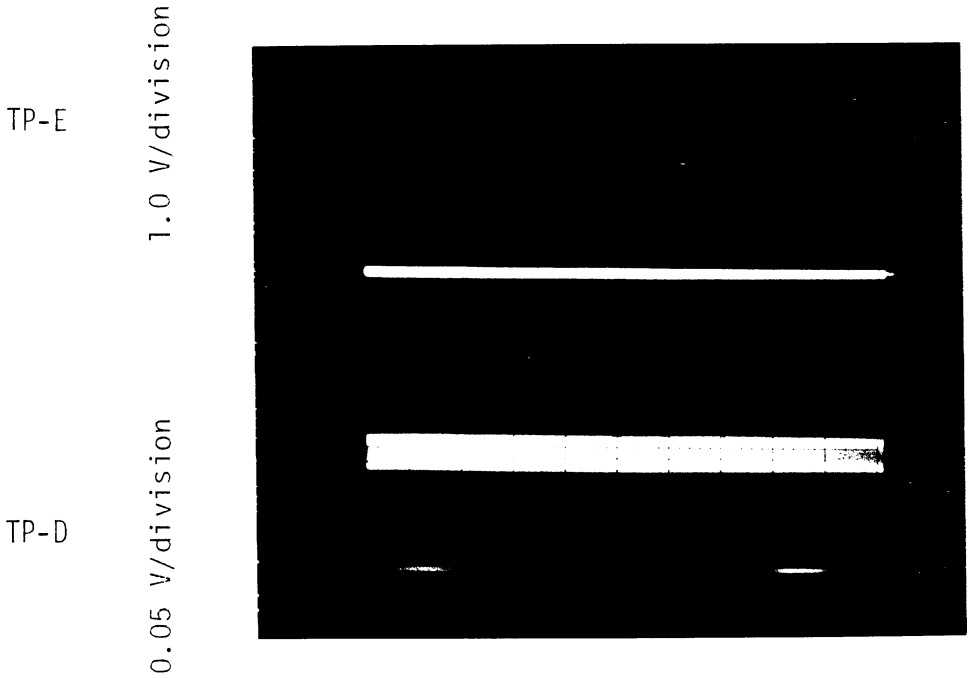

Figure 27. Signals at test points E and D with reduced amplitude (-20 dB) short pulse plus RF carrier input. RF carrier amplitude = 5000 μV.

The effects of the introduction of RF carrier signal at the input can be identified clearly by comparing the signals at E shown in Figs. 22 and 23. Figures 23 through 26 show the signals at test points D and E, with an input signal consisting of a variable amplitude RF carrier and a constant amplitude short pulse signal. Observe that as the carrier level is increased, the audio pulse output (i.e., E signal amplitude) is decreased--this indicates that the existence of carrier tends to suppress the audio effects caused by the input short pulse. Results shown in Fig. 27 were obtained under conditions similar to those in Fig. 24, but with a short pulse having 20 dB less amplitude; the results of Figs. 25 and 27 indicate that with a given RF carrier and variable amplitude short pulse signal, the audio output signal amplitude varies directly with the input short pulse amplitude.

3.4.4 Role of Pulse to Carrier Ratio at the Input. Results given in Section 3.4.3 indicate that with an input consisting of RF carrier plus short pulse signals, the audio noise output from the test radio caused by the short pulses depends significantly on the amplitude of the RF carrier at the input and, in particular, on the pulse to RF carrier amplitude ratio at the input. We have also seen that at the test point E and at the audio amplifier output [Fig. 15] there always exist a certain amount of signals caused by a given input pulse, although its amplitude decreases as the RF carrier level at the input is increased. Existence of these signals at test point E and at the audio amplifier output does not necessarily mean that there would be audible noise output from the speaker; the above signals must be strong enough for the speaker to

produce perceptible noise. Therefore, it is of practical importance to know under what conditions, a given short pulse input would produce audible noise at the test radio output.

To this end, the test radio was adjusted for standard test conditions; the input RF carrier (100 MHz, 1 kHz modulation frequency) and the short pulse (τ = 10 ns, repetition rate 100 Hz) inputs were then adjusted for threshold noise output from the speaker. The signal amplitude at test point E at the oscilloscope, as well as the RF carrier and pulse amplitudes at the input (at TP-A) were noted. Next, the RF carrier level was increased by a certain amount; this caused the TPE signal level as well as the noise ouptut from the speaker to go down. The input pulse amplitude was then increased so that the TPE signal amplitude (and the audio noise output) assumed the previously obtained threshold level. The new amplitudes of the RF carrier and short pulse signals at the input were noted. The process was repeated for selectively increased values of the RF carrier amplitude at the input. The results are shown in Table 7 where the last column gives the pulse to carrier amplitude levels at the input required to produce threshold noise.

Table 7

RF Carrier and Pulse Amplitude Levels at the Input (TPA) Required for Threshold Noise Output

RF Level(μv)	Pulse Level (V)	Pulse/Carrier = S
5	0.02	4000
24	0.09	3750
80	0.26	3250
240	1.00	4166
806	2.60	3226
2400	9.00	3750
8000	26.00	3250
24000	90.00	3750

The results of Table 7 show that the pulse to carrier amplitude ratio (S) at the input required for producing detectable noise at the output stays almost constant for all the RF carrier amplitudes considered. Thus, we take the average value of the last column of Table 7, i.e., $S_{av} \simeq 3650$ (or ~71 dB) as the threshold value for the test radio. This would mean that with a given input RF carrier level of 10 μV, an input pulse (10 ns wide) of amplitude $10 \times 10^{-6} \times 3650 = 36.5$ mV would produce detectable noise at the output; of course, pulses having amplitude $\geq$ 36.5 mV would produce more noise.

With the same RF carrier and pulse input signals to produce threshold noise at the output, as discussed above, the carrier to pulse ratios were also measured at the test point B. For the input signals given in Table 7, it was found that the carrier to pulse ratio at B remained approximately the same as given in Table 7.

3.5 Discussion

On the basis of the results discussed above, the following general comments are made with regard to the susceptibility of automobile radios to input impulsive noise signals.

(i) The response of an automobile radio to impulse or short pulse input signals depends significantly on whether or not an RF carrier signal exists at the input. Generally, the existence of an RF carrier signal tends to reduce the overall effects of the pulse, the amount of reduction is determined by the level of the carrier relative to that of the pulse.

(ii) The tunable filter at the front-end of the radio selects the frequency component of the pulse corresponding to the frequency to which

the radio is tuned. With a given short pulse input and the radio adjusted to standard test conditions, it has been found that the audio noise output as a function of the tuning frequency varies inversely as the spectral amplitude distribution of the pulse. As a result, the amplitude of the input pulse as a function of tuning frequency required to obtain a constant audio noise output assumes a maximum value at the frequency where the input pulse has a missing spectral component. For an input pulse of width $\tau \leq 8$ ns (i.e., no missing spectral component within the FM-band frequencies) and repetition rate 100 Hz, typically a pulse amplitude of 0.005 V is required to produce threshold noise at the output.

(iii) With an RF carrier signal present, significantly larger amplitude pulse signal is required to obtain the same threshold audio noise output. It has been established that with a given level of RF carrier signal at FM frequencies, threshold noise at the output is produced if the input short pulse has a typical level of about 3650 times (or ~71 dB larger) than that of the carrier.

Ignition pulse signals at the antenna terminals of Ford cars being of the order of 50 mV, it is argued that the FM reception of the radios would be susceptible to ignition noise if the received signal voltage at the radio input is $\lesssim 14$ μV. Ignition pulse generated voltage at the antenna terminals of the Monte Carlo being 400 mV, the susceptibility of the radio on the Monte Carlo would occur for signal voltage levels ≤ 102 μV.

(iv) The pulse responses of radios do not depend significantly on the pulse repetition rate; however, they do quite strongly on the pulse width--radios become more susceptible to shorter pulses.

(v) All radios tested appear to respond similarly to similar input signals--no significant difference in performance has been found from radio to radio.

IV. USE OF PROBES FOR RFI FIELD MEASUREMENTS

The present chapter describes the results of an investigation carried out to explore the possibilities of using field probes or sensors to measure the fields, on or near the surface of a vehicle, and created by the vehicle ignition system. Such probes have been used in one of our previous automotive studies [3], and also in a study [ ] of the surface fields on various conducting bodies induced by plane electromagnetic waves.

4.1 The Field Probes: Calibration Procedure

Two electrostatically shielded loop type of probes, similar to current sampling loops used in antenna measurements [7], were fabricated from coaxial lines formed into loops of desired diameters. Figure 28 illustrates the fabrication process. The diameter of each loop was chosen to be less than 0.0625 λ at the operating wavelength λ so as to obtain a near uniform distribution of current along the circumference of the loop. The coaxial transmission line employed was fabricated from uniform tube wire, and is designated as UT-141P. The diameter of the two loop configurations were 3.0 inches ($\sim$0.025 λ at 100 MHz) and 1.0 inch ($\sim$0.008 λ at 100 MHz).

The sensitivities of the above ten probes were determined by far field measurements carried out in an 80-foot ground plane range.

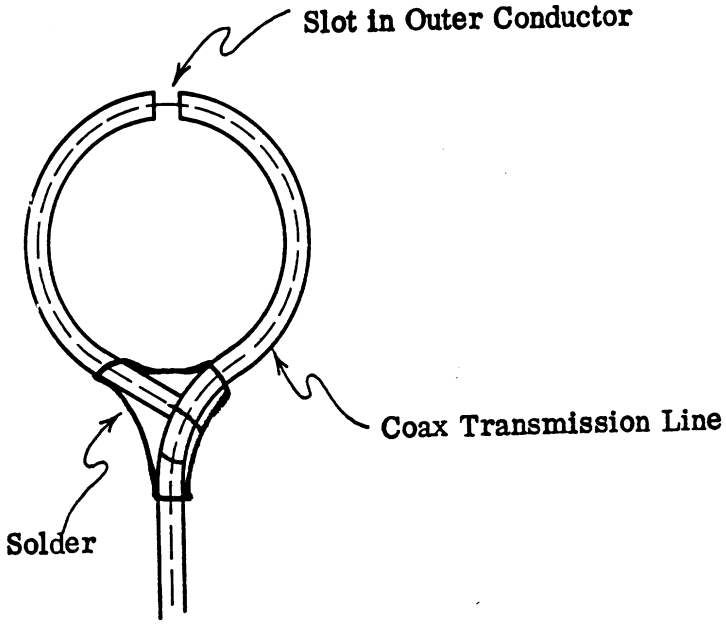

Figure 28. Diagram showing the construction of a shielded loop used as field probe or sensor.

The measurements were carried out as follows. The height of the field probe (i.e., the loop) was fixed at a height of 8 feet, and that of the transmitting antenna was varied between 12.5 feet and 50 feet depending on the frequency of operation. The height of the transmitting antenna was varied to ensure that the direct and ground-reflected fields were in phase at the location of the field sensor. With the geometry of the field probe, and the transmitting antenna with respect to the ground as shown in Fig. 20, it can be shown that the two fields would be in phase if the following relationship is satisfied:

$$h_r = \frac{\lambda R}{4h_t} , \quad .... \qquad (5)$$

where all the parameters involved are as explained in Fig. 29. Figure 30 shows the details of the experimental set up used to calibrate the test probe by far field measurements.

The probes were calibrated between 50 and 200 MHz and at 10 MHz intervals. The incident field was at first measured with a $\lambda/2$ dipole, and then with each of the field probes. The fields received by the dipole and the two probes, normalized to the field received by a $\lambda/2$ probe, are shown in Fig. 31. In addition to the measured results, a theoretical curve for the 3.00 inch loop obtained from [7] is also shown in Fig. 31 which indicates good agreement between theory and experiment.

Based on the results shown in Fig. 13 and other tests carried out, it was decided that the 1.00 and 3.00 inches diameter probes be

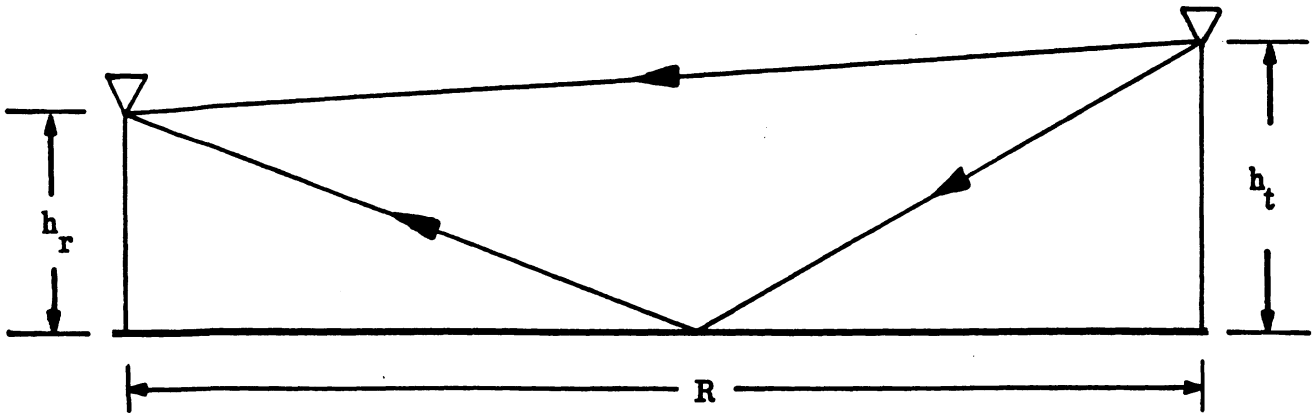

Figure 29. Geometry of the field sensor and the transmitting antenna located above ground.

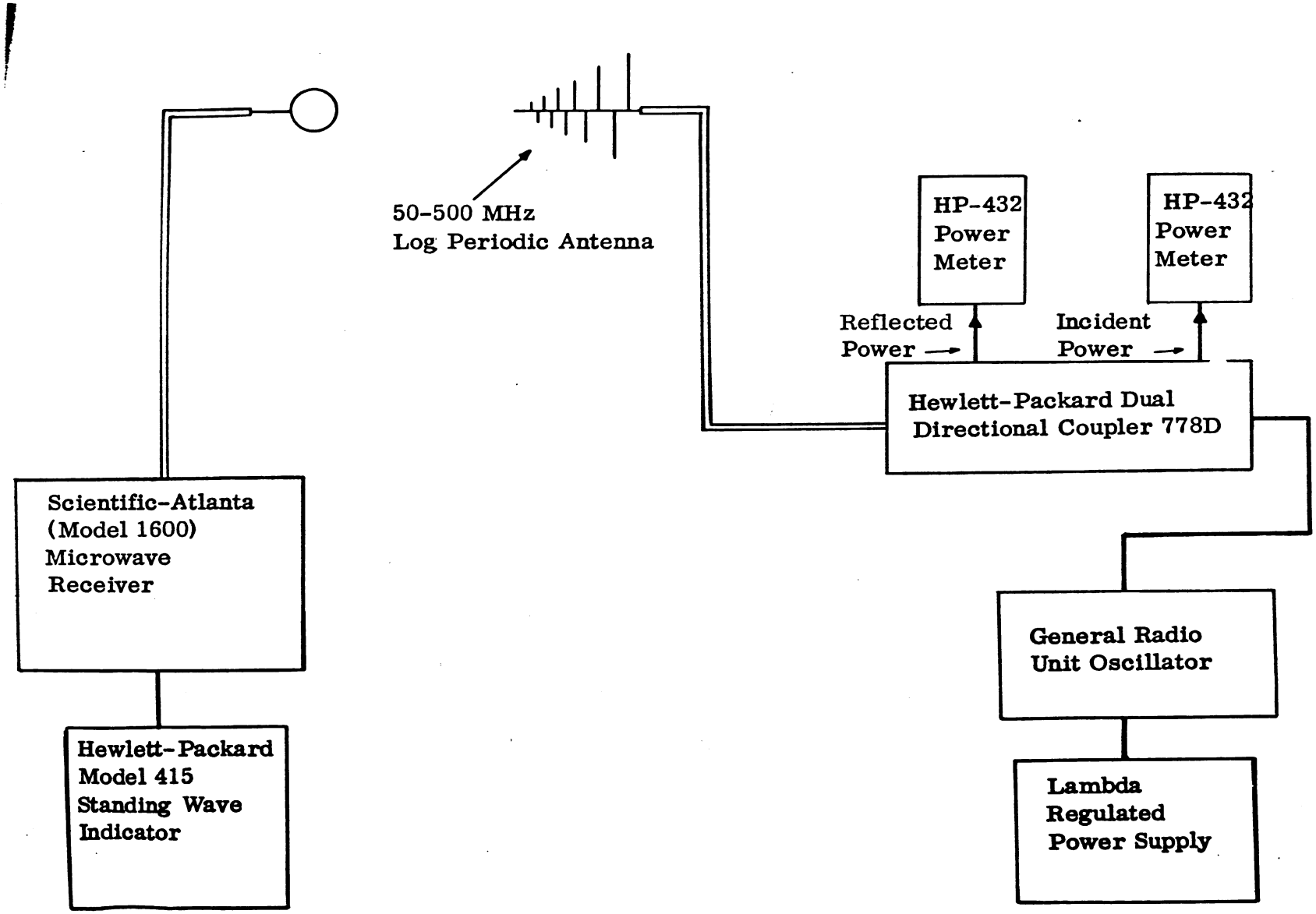

Figure 30. Block diagram of the equipment set-up used for far field calibration of the loop.

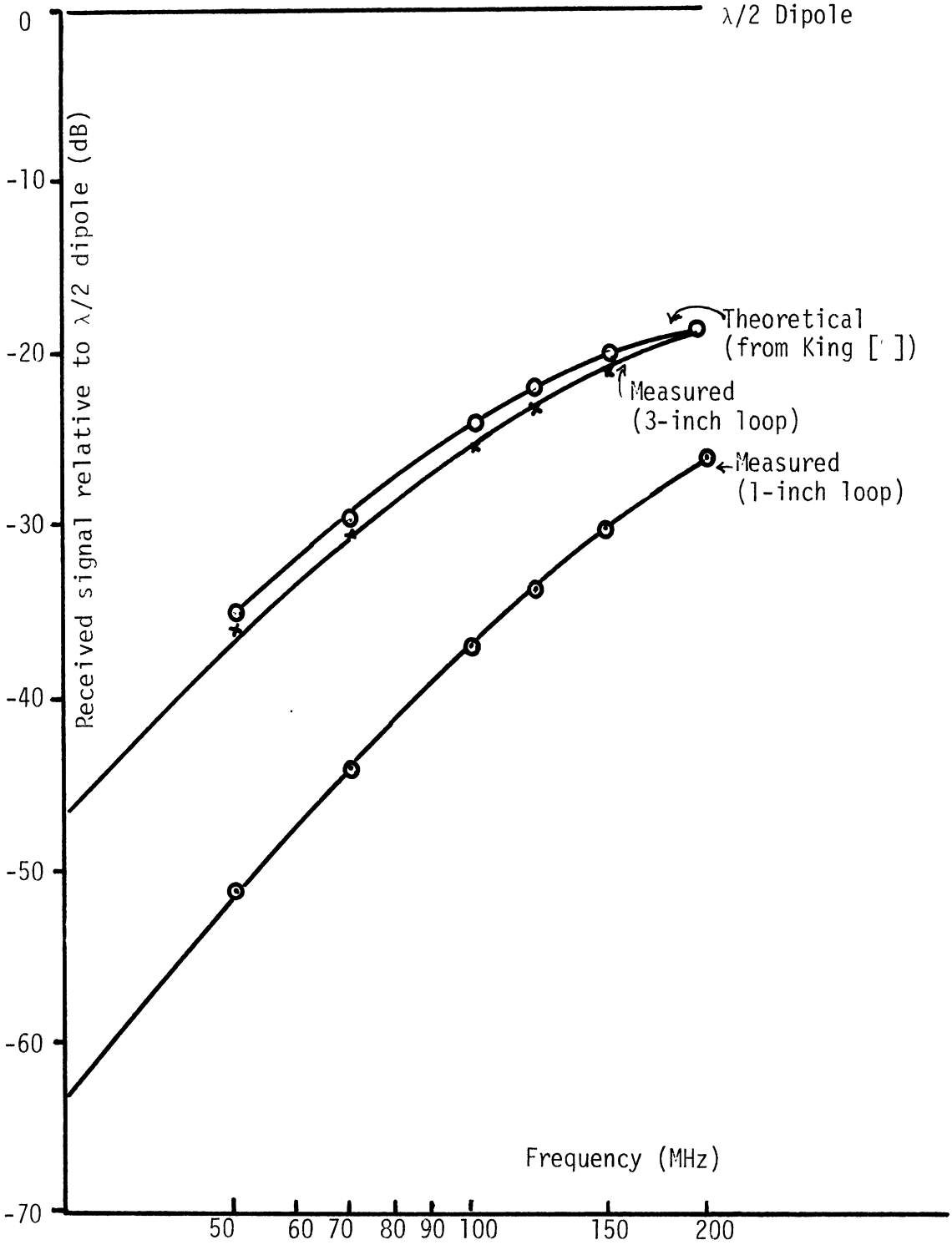

Figure 31. Calibration curves for the probe relative to λ/2 dipole.

used to make the quasi-conductive and near field measurements, respectively. The former measurements were made with the sensor in contact with the surface area under test, and the taller were made with the sensor located in the vicinity of (but not touching) the surface area under evaluation.

Initial field probings were carried out with the field sensors attached to either a Hewlett-Packard 8558B/182T spectrum analyzer or a Singer NF205 RFI meter. For both quasi-conductive and near field measurements, results were found to be more reliable with the Singer instrument. Therefore, it is recommended that a Singer NF205 RFI meter or an equivalent RFI instrument be used for such future measurements.

4.2 Techniques of RFI Field Measurement

Three schemes of measurements, based on the metered slideback method described in Appendix A, were investigated to measure the RFI signals received by the field sensors. First, in the meter needle deflection method, the received signal was monitored by following the deflections of the receiver meter needle. Second, in the aural method, a set of earphones was used to monitor the interference signal. Third, in the visual method, the received RFI signal was monitored on an oscilloscope screen. Repeated tests showed the meter needle deflection method to be unsatisfactory because the data exhibited poor repeatability. Although the visual method produced acceptable results, it was found necessary to use the aural technique as an additional aid to ensure data repeatability. Therefore, it was decided to use the aural scheme to obtain the desirable data.

Because of the difficulties involved in obtaining valid data in RF noise measurements, some precautions are necessary to ensure data integrity. The operator should experiment extensively with the particular receiver associated with the sensor and thereby develop a feeling for the validity of the data collected. Care should be taken to assure that the automobile engine under evaluation has reached a steady state, before the measurements are performed; thus many erratic results may be avoided. To minimize the randomness of the RFI data collected, it is suggested that the engine speed be set at 1000 rpm.

4.3 Quasi-Conductive Data

As mentioned earlier, quasi-conductive measurements were performed by making physical contact between the sensitive area of the probe (i.e., the surface around the gap) and the cable or other pertinent surfaces where the RFI fields were to be measured. For example, the loop was in physical contact with the insulation on wires, and to assure maximum signal pick-up by the loop, the plane of the loop was placed parallel with the cable, i.e., parallel to the electric current induced in the cable.

The chief purpose of making the quasi-conductive measurements was to obtain the induced fields on the isolated parts of various components; therefore, care was taken to shield or move away from other RFI radiation so as to isolate the component under test. Further discrimination against adjacent RFI radiation was achieved by using the 1.0 inch loop during the quasi-conductive measurements.

Figures 32 and 33 illustrate some typical results obtained from a Ford vehicle. Figure 32 shows the RFI signal amplitude as a function of frequency obtained at one of the alternator wires; the observed amplitude variations with frequency in Fig. 32 were found to be much greater and more erratic than those obtained with most other components investigated. Figure 33 shows the RFI field strengths adjacent to the left rear (as viewed from the front of the vehicle) spark plug wire obtained with the vehicle hood open and closed. The results indicate that the opening or closing of the hood had negligible effects on the existing RFI fields.

4.4 Near Field Data

Near field measurements were carried out by placing the probe within a distance of two wavelengths from the object under test. In the frequency band of interest, i.e., 50 to 200 MHz, the near field region extends several feet from the test car body.

The vehicle ignition system generated electromagnetic pulses may, in general, induce currents on the entire body of the car in a random fashion. Therefore, during the near field measurements it was necessary to vary the plane of the probe to maximize its response.

All near field data were obtained with the 3.00 inch probe, and are shown in Figs. 34 through 40. Figure 34 shows typical results obtained with the loop located near the slot between the hood and the car body and just above the right front tire (as viewed from the driver's seat). The RFI field detected with the plane of the loop perpendicular

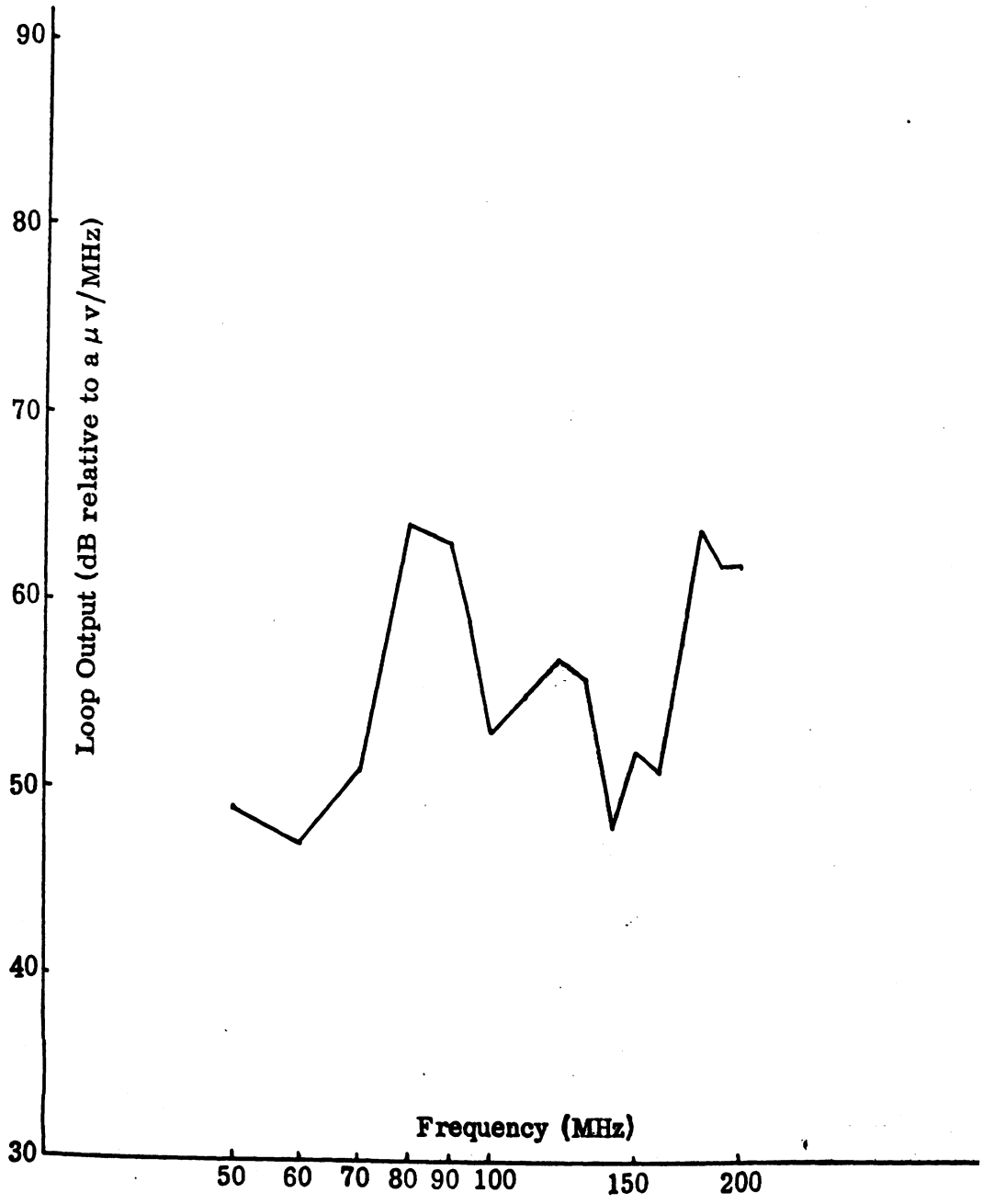

Figure 32. Quasi-conductive measurement results obtained with 1.0 inch loop probe adjacent to the alternator wire. Test car: Ford LTD.

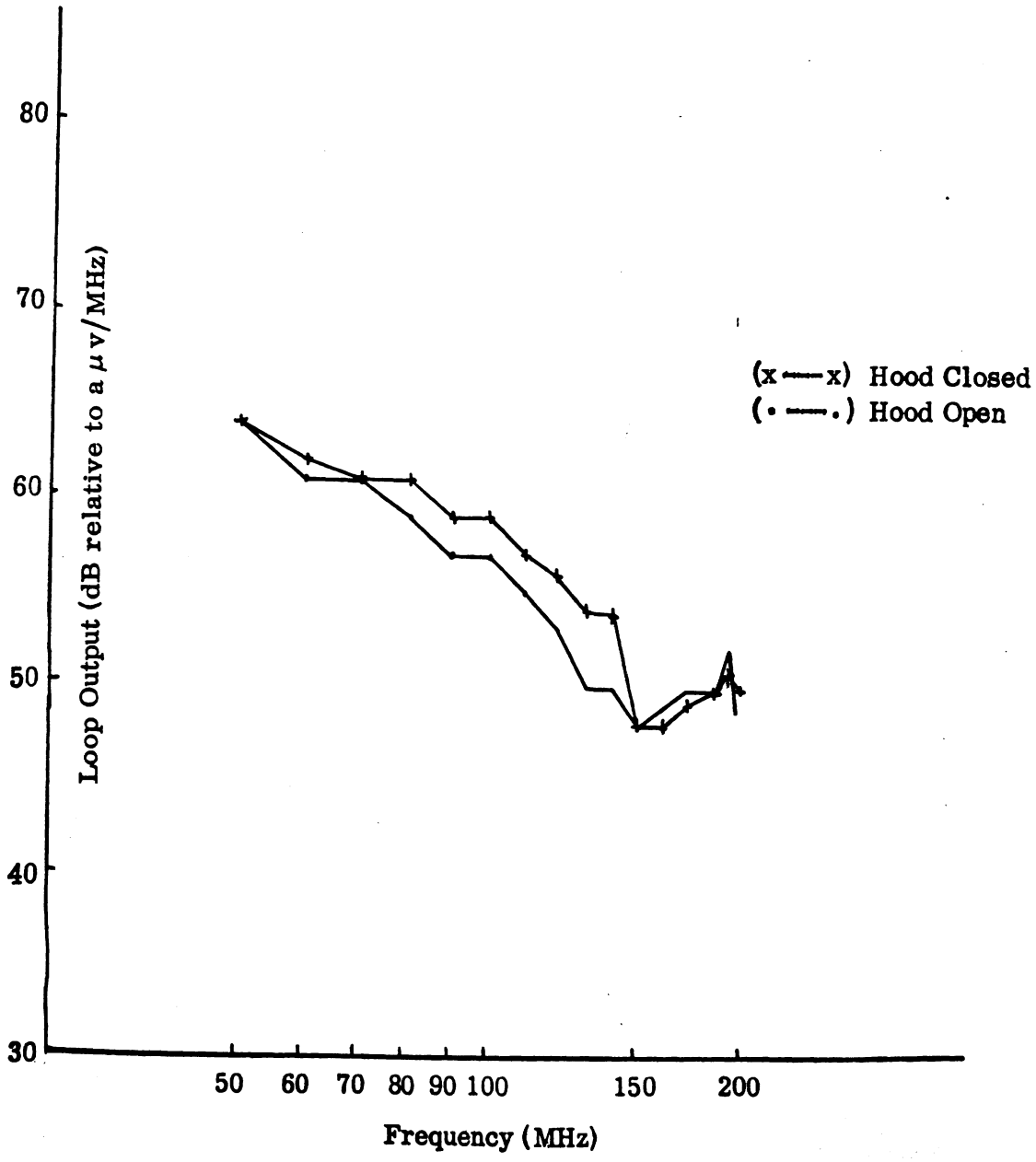

Figure 33. Quasi-conductive measurement results obtained with 1.0 inch loop probe adjacent to the left rear spark plug wire with the hood open and closed. Test car: Ford LTD.

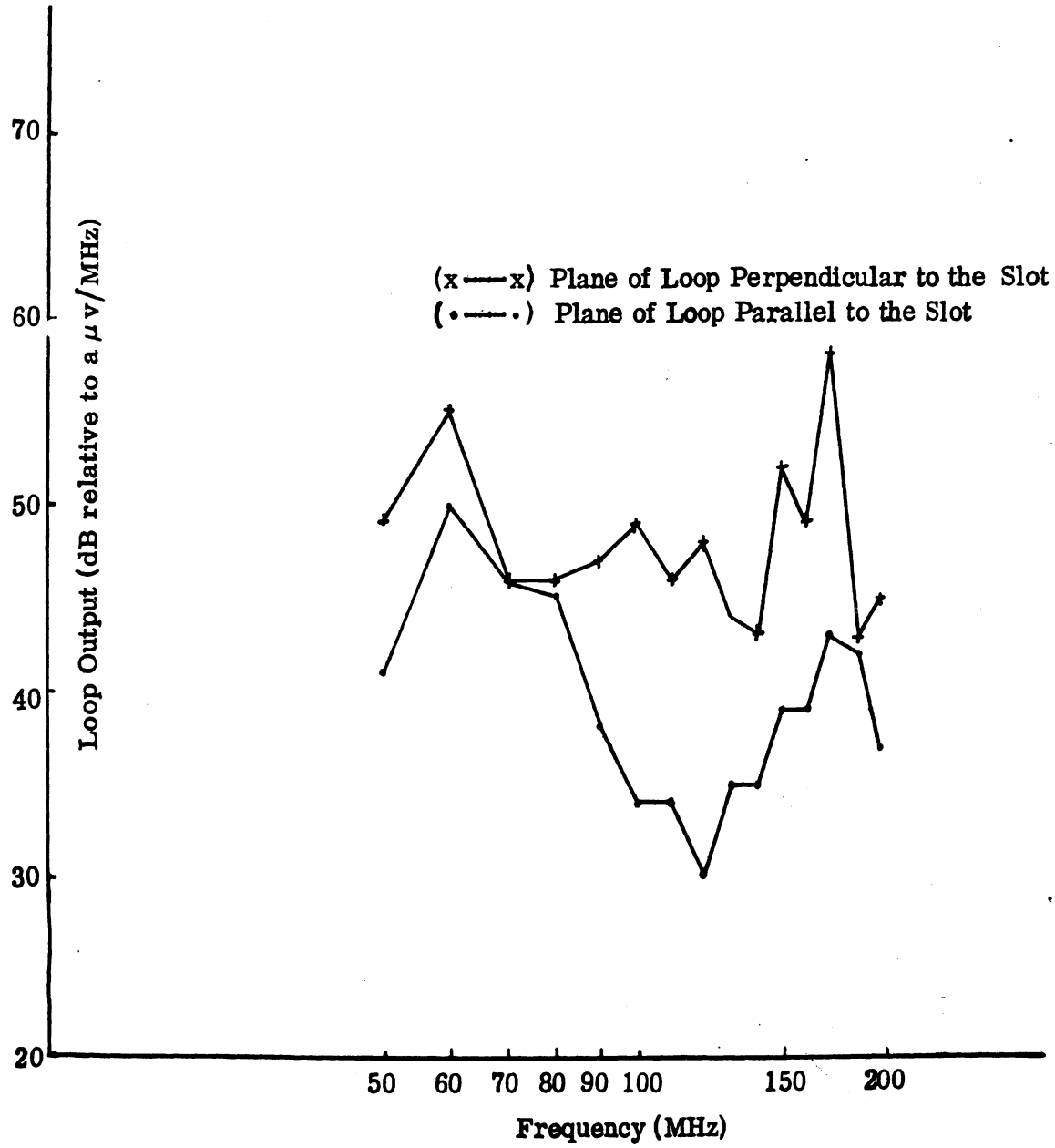

Figure 34. Near-field results obtained with 3.0 inch loop probe placed 3 inches above the slot between hood and car body above right front tire. Test car: Ford LTD.

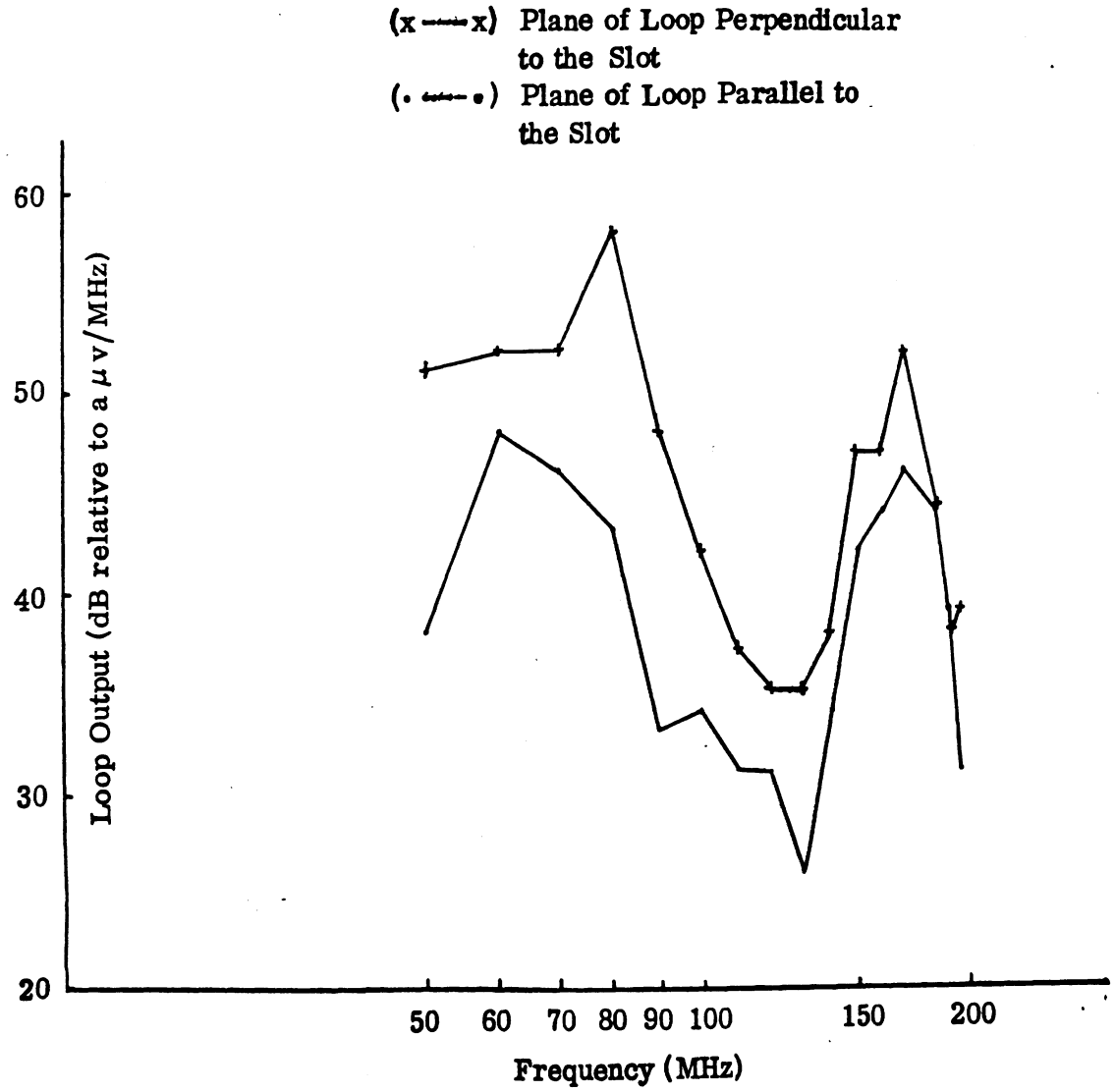

Figure 35. Near-field results obtained with 3.0 inch loop probe placed 3 inches above the slot between front hood and car body and next to the radiator. Test car: Ford LTD.

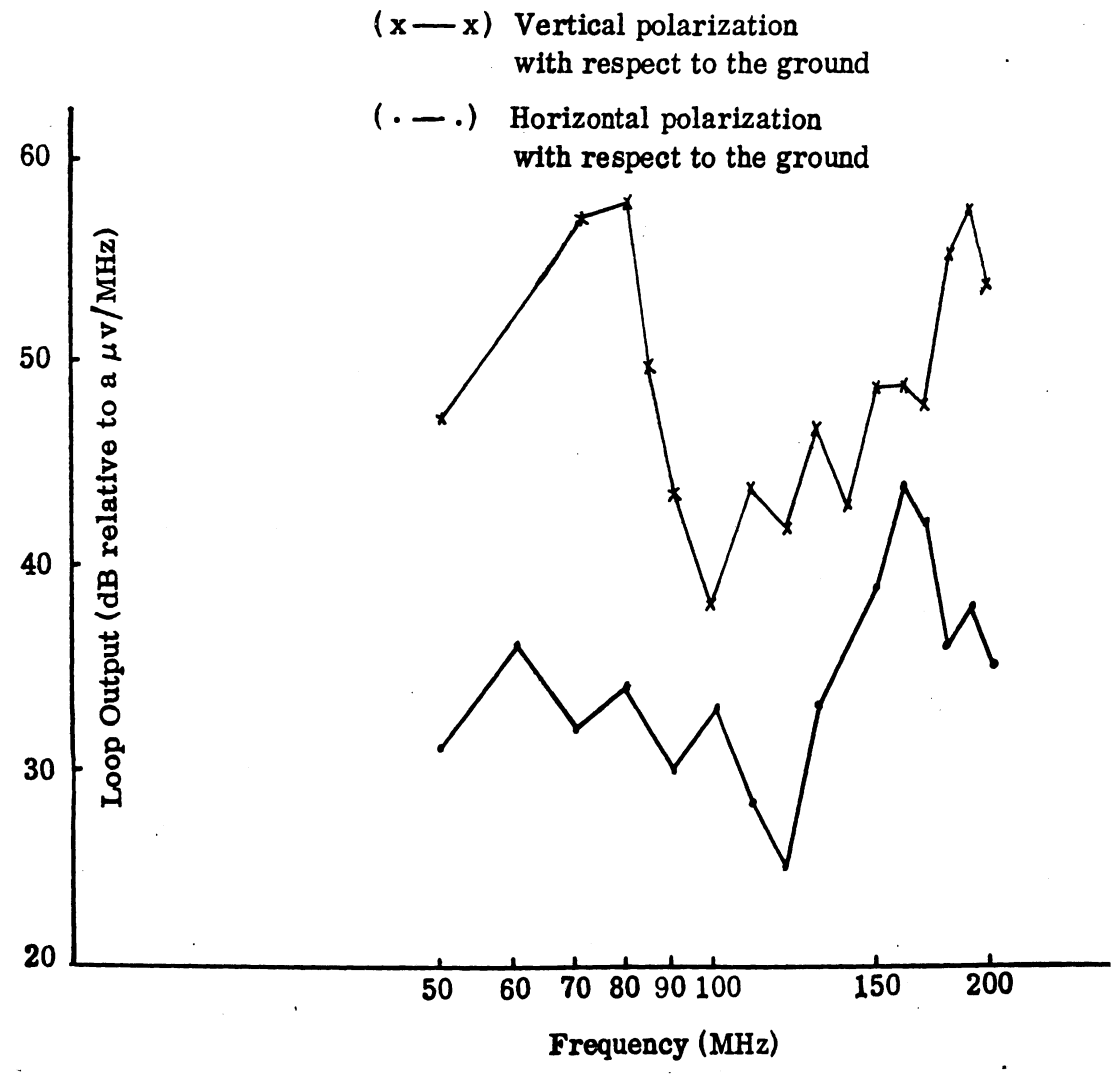

Figure 36. Near-field results obtained with 3.0 inch loop probe 4 inches away from right front tire and 2 feet above ground. Test car: Ford LTD.

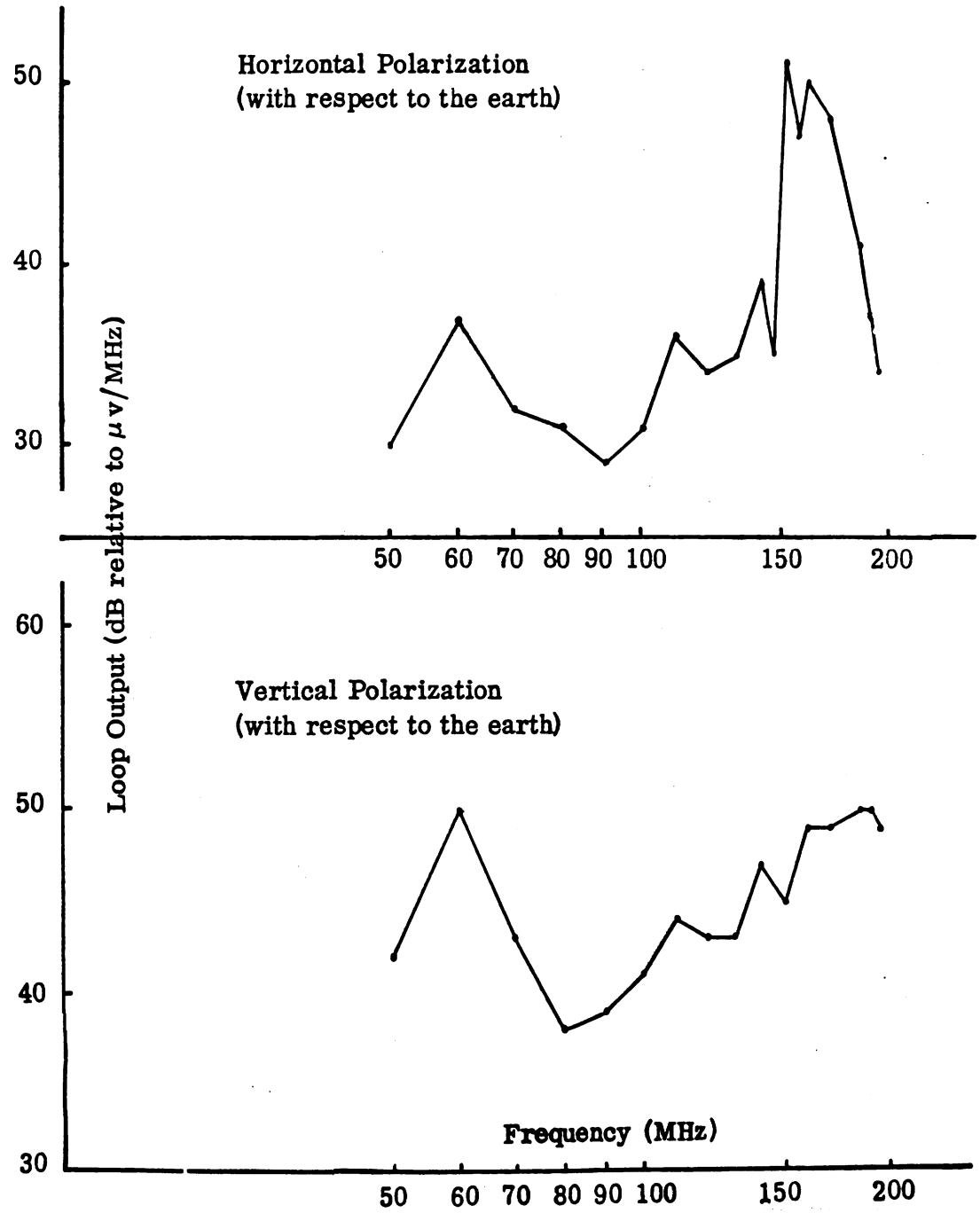

Figure 37. Near field results obtained with 3 inch loop probe 4 inches away from left front tire and 2 feet above ground. Test car: Ford LTD.

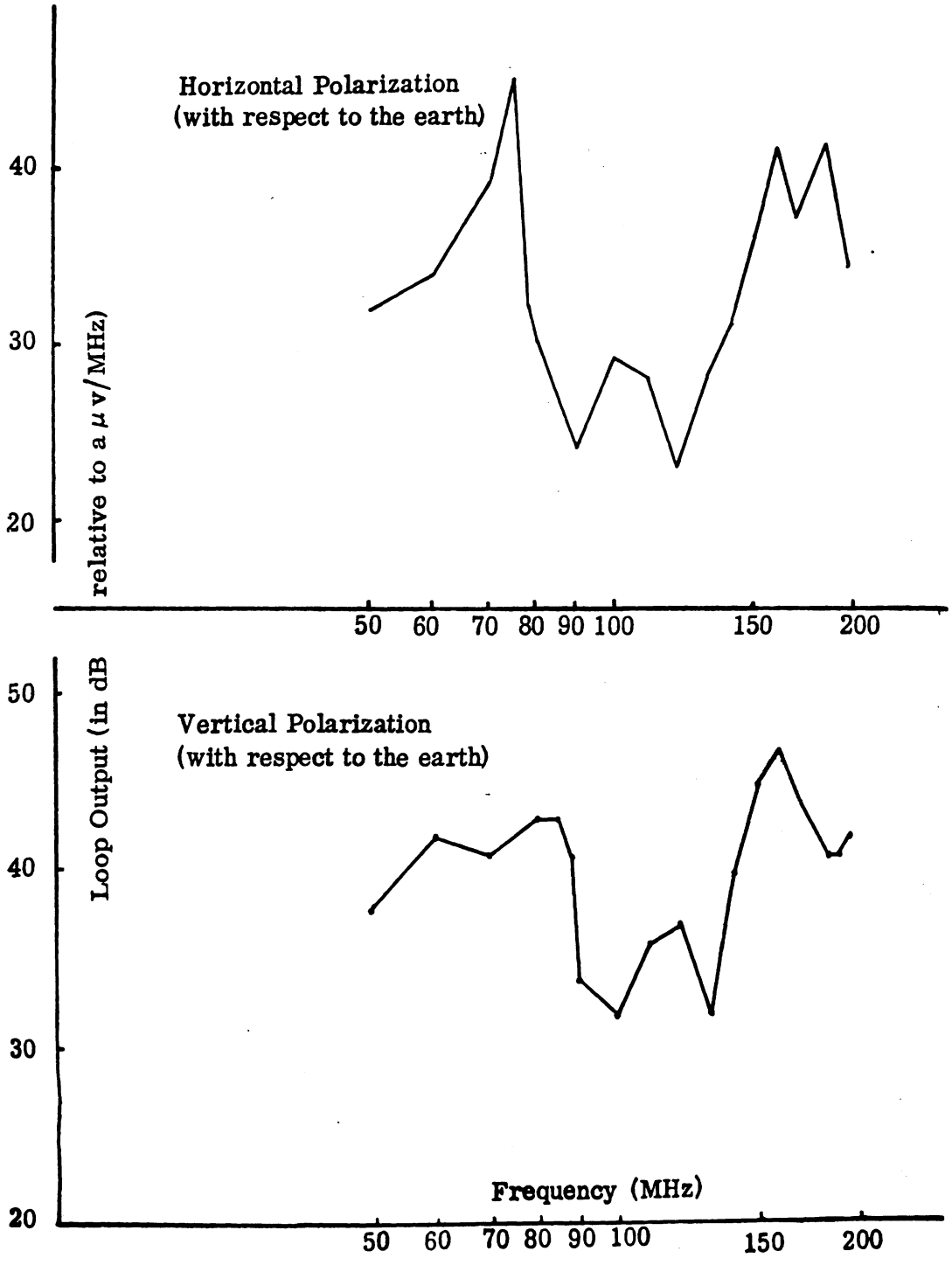

Figure 38. Near-field results obtained with 3 inch loop probe 12 inches away from center of front gripp and 2 feet above ground. Test car: Ford LTD.

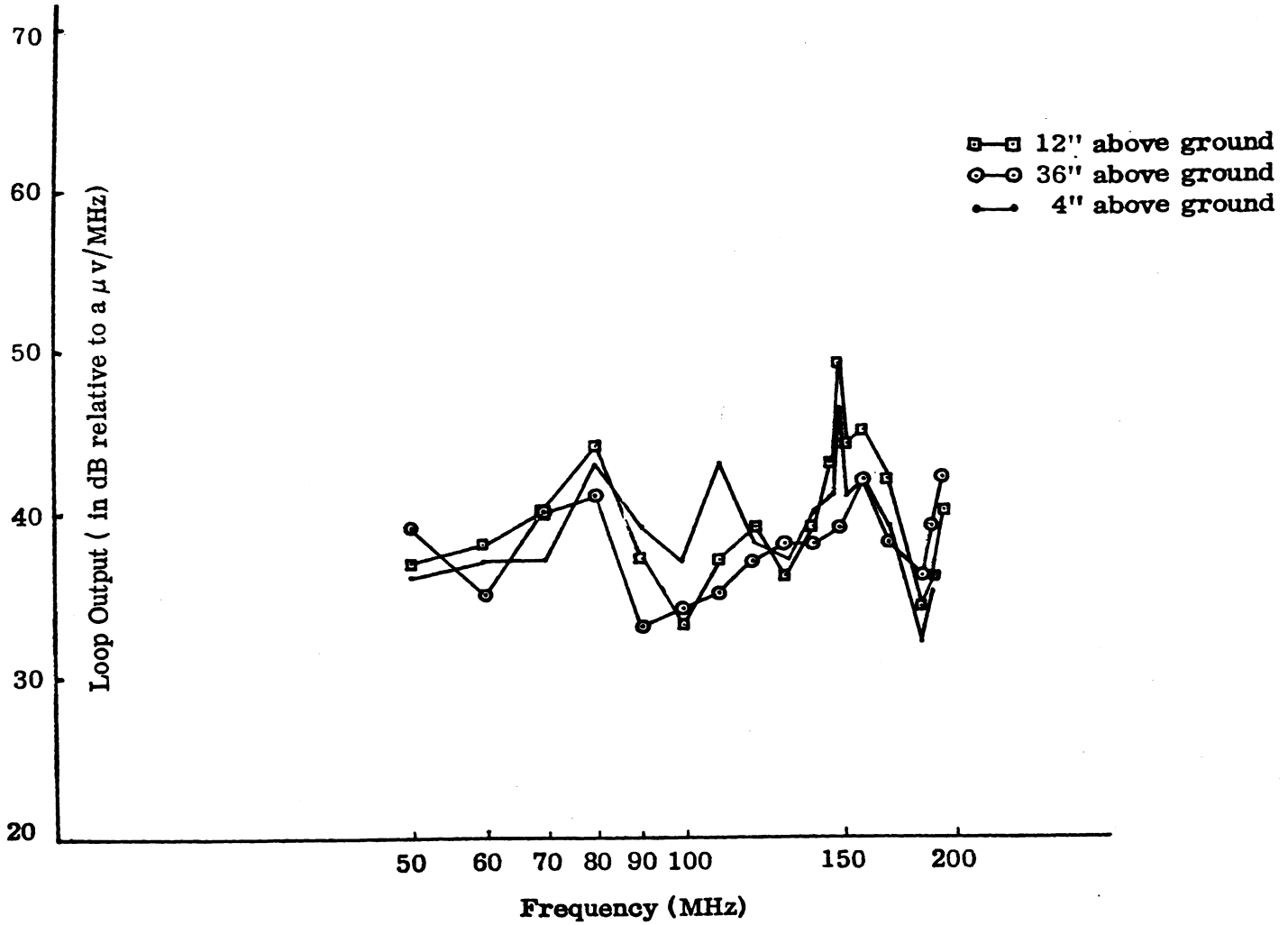

Figure 39. Near-field results obtained with 3 inch loop probe 12 inches away from center of grill and positioned at various heights above ground. Vertical polarization. Test car: Ford LTD.

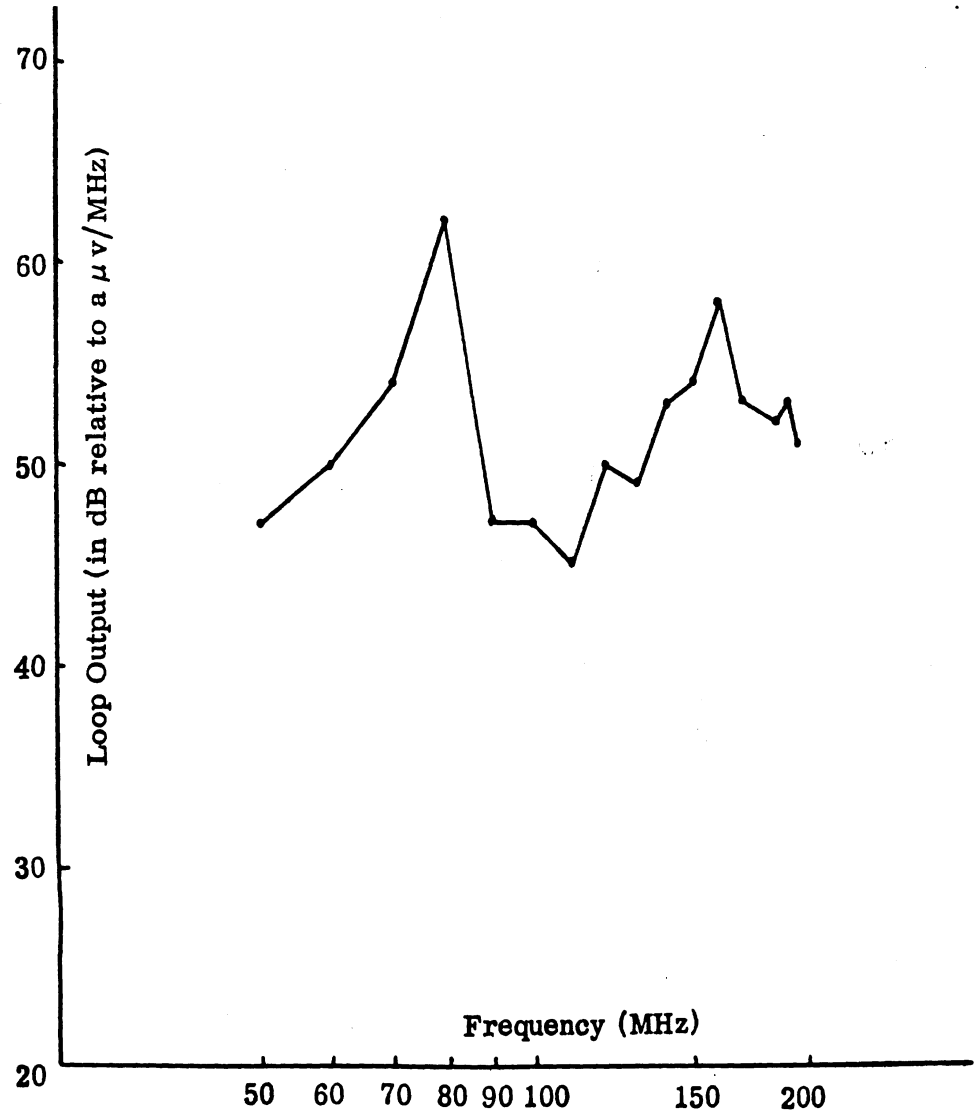

Figure 40. Near-field results obtained with 3 inch loop probe placed 20 inches above the car air filter and with hood open. Loop positioned for vertical polarization and oriented in azimuth for maximum recieved signal. Test car: Ford LTD.

to the slot tends to be larger (Fig. 33). This may be expected, since the E-field in the slot would be across the slot while the H-field component would be parallel to the slot. Similar results in the slot region obtained with the probe placed above the center of the front hood area are shown in Fig. 35. The same observation, with respect to the plane of the loop (i.e., the polarization of the detected field) can also be made here. Note that in Figs. 34 and 35, and also in subsequent figures, the measured field intensity exhibits a minimum near 100 MHz. As noted previously (Section 3.3.1) this minimum is believed to be related to the missing frequency component (near 100 MHz) of the 10 ns ignition pulse.

Figures 36 and 37 show the RFI fields measured 4 inches from the right and left front tires, respectively, and at a height of 2 feet above ground. In both cases, the vertically polarized fields tend to be slightly larger which is expected in the vicinity of a conducting ground plane.

Figure 38 shows the results obtained with the probe located 12 inches in front of the grill and 2 feet above ground; these results appear to be similar to those in Figs. 36 and 37. The results shown in Fig. 39 show the vertically polarized E-field measured with variable heights of the probe above ground. The results indicate that over the frequency range 50 to 200 MHz and with the heights used, the E-field was relatively constant, as may be expected.

The final set of results, shown in Fig. 40, was obtained with the probe located 20 inches above the vehicle air filter and with the hood open. During this measurement the plane of the loop was oriented

vertical with respect to the ground, and perpendicular to the center line of the test car. The most significant observation from the results shown in Fig. 40 is that the measured field strengths are appreciably larger than those shown earlier; this is expected, since these results were obtained with the vehicle hood open.

4.5 Discussion

The results presented above indicate that the vehicle generated RFI fields on or near its surface can be measured using the field probes or sensors. Quasi-conductive and near-field type of measurements were investigated: The former yields results which may be used to estimate the surface fields, and the latter can be used to determine the fields existing in the desired vicinity of the test car.

Shielded electrostatic loops have been found useful to sample the RFI fields. Two such loops having 1-inch and 3-inch diameters were fabricated and used to collect various results. On the basis of the results obtained it is recommended that the quasi-conductive and near-field measurements be carried out with the one-inch and three-inch diameter loops, respectively. For obtaining reliable and consistent results, it is suggested that the Singer NF205 or an equivalent RFI meter be used along with these loops.

Of the three schemes of RFI field measurements investigated, the aural scheme was found most dependable and, hence, is recommended for such future measurements.

APPENDIX A

MEASUREMENT OF BROADBAND QUASI-CONDUCTED OR NEAR-FIELD RADIATED SIGNALS BY THE METERED SLIDEBACK METHOD

The directions in the Singer NF 205 RFI manual that apply to the quasi-conductive and near-field measurements of the radiation from automobiles are sometimes difficult to follow. This is partly because some appear in one place and others in another place in the manual. In addition they seem imcomplete and unclear when applied to these particular measurements. For these reasons we have prepared a revised set of instructions describing the procedures which we found to be satisfactory.

It may be well to restate the principle on which the operation of the Singer NF 205 RFI meter is based. Briefly, it is as follows. The signal to be measured is detected and amplified and its intensity is indicated on the meter or by the sound level in the earphones. Dial settings give information on the frequency. Attenuation is introduced by means of calibrated attenuators to reduce the indicated signal to the threshold of audibility (or to some other suitable indication, e.g., visual). At this stage, the unknown signal is switched off and the output of the calibrated impulse generator which is a part of the RFI unit is fed through the same circuits used in the detection, amplification and attenuation of the unknown signal. The output level of the impulse generator is adjusted until its aural indication is just barely at the threshold of audibility. Assuming no change in the attenuator setting and assuming a reliable calibration on the impulse generator, the level of the unknown signal is that which is indicated on the dial of the impulse generator in dB above 1 μv/MHz.

RF energy radiated from an internal combustion engine tends to be erratic and non-repetitive causing the response of the metering circuitry of the output meter pointer to fluctuate, thereby making measurement difficult. To measure such signals accurately, the metered slideback technique provided with the Singer NF 205 RFI meter should be employed. To make the measurements in the 50 - 200 MHz frequency range the T-1/NF-205 tuning unit is used. Aural monitoring of applied signals is highly desirable and earphones should be plugged into the PHONES receptable. The loudness of the aural indication can be adjusted to a comfortable level by means of the VOLUME control.

Many of the instructions, a through q, which follow have been lifted verbatim from the Instruction Manual of the NF-205 RFI meter.

a. Apply power and perform the preliminary adjustments as noted below.

1. Initial Control Settings. Set the controls as listed in Table 1 prior to application of line power. Controls not specifically referenced in the table may be set set to any arbitrary position.

2. Power Application and Preliminary Adjustments. To prepare the NF-205 for operation, proceed as follows.

With the POWER Switch set to OFF, check the indication of the output meter pointer; it should indicate 0 on the MICROVOLTS scale. If this indication is not obtained, carefully adjust the output meter mechanical zero set screwdriver control until the pointer deflects to a MICROVOLTS scale indication of 0.

CAUTION

PULL OUT THE SIGNAL ATTENUATOR DB SWITCH BE-
FORE PLACING IN A NEW SETTING. TURNING THE

SWITCH KNOB WITHOUT FIRST PULLING IT FORWARD WILL DAMAGE THE SWITCH. AFTER THE DOT ON THE SWITCH KNOB IS LINED UP FOR THE DESIRED SETTING, PUSH THE KNOB ALL THE WAY IN.

TABLE 1: INITIAL CONTROL SETTINGS

Control	Setting
POWER switch	OFF
METER switch	INT
CAL switch	SHUNT
SIGNAL ATTENUATOR DB switch	20
IMPULSE GENERATOR switch	OFF
IMPULSE GENERATOR DB ABOVE 1μV/MHz switches	10 and 0
GAIN control	Mid-range
VOLUME control	Mid-range
Function Selector switch	ZERO ADJ
METER DAMP switch	OFF
SLIDEBACK control	Fully clockwise
ZERO ADJ control	Mid-range

After the preliminary adjustments have been performed, determine the type of measurement to be made (quasi-conductive or near-field radiation). Connect the appropriate pickup device (3/4" loop for conductive measurement and 3-3/4" loop for near field radiation measurement) and auxiliary equipment to the basic unit and/or tuning unit as illustrated in Figure A-1.

Interconnect the equipment as illustrated in Figure A-2. Set the POWER switch to ON and, if an inverter or autotransformer is employed, set its "power" switch to "on". If an autotransformer is employed, adjust its output for 115 volts after it stabilizes. The POWER pilot lamp will illuminate upon application of the line power. Allow the equipment to warm up for at least 15 minutes.

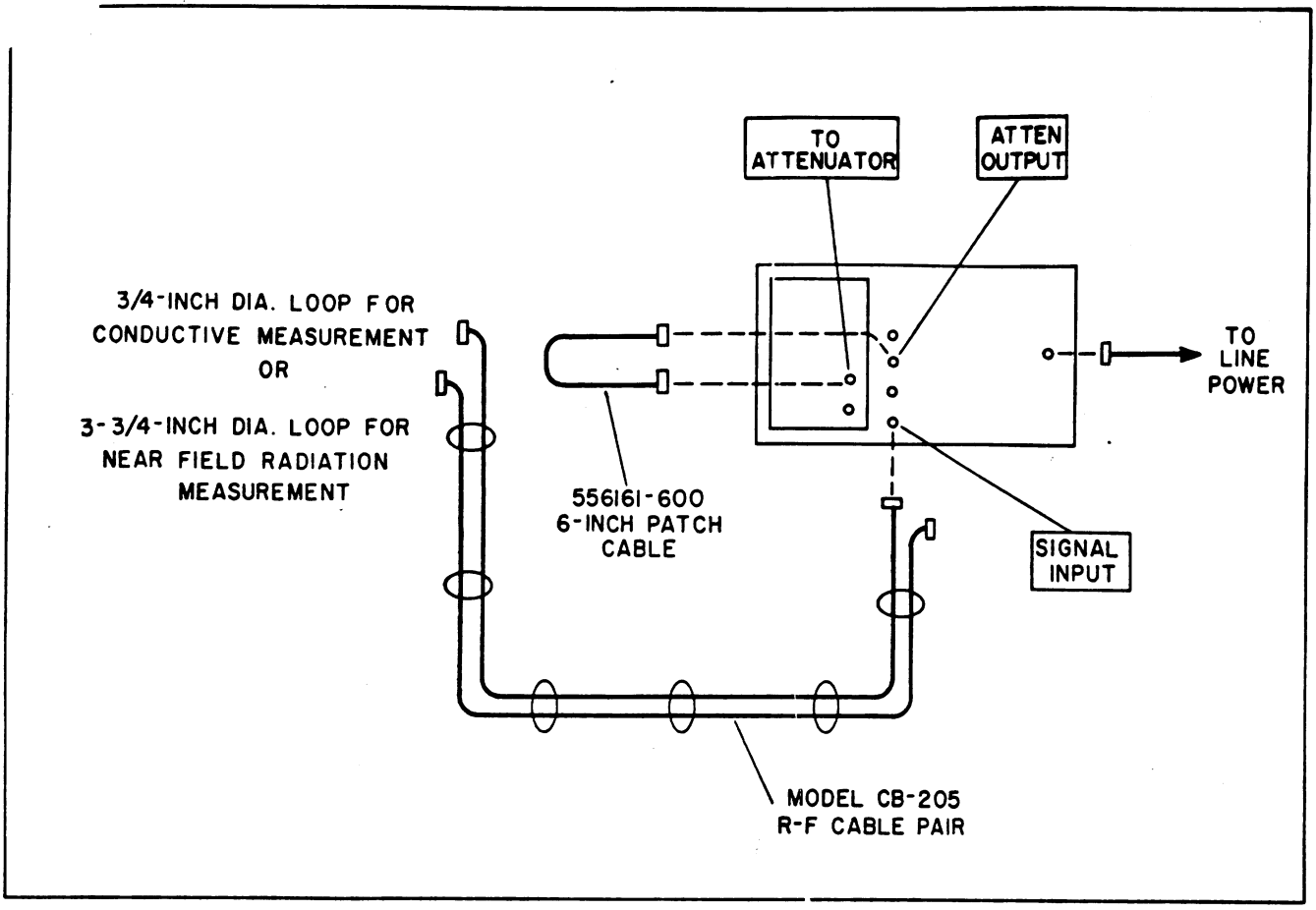

FIGURE A-1: BASIC INTERCONNECTION DIAGRAM

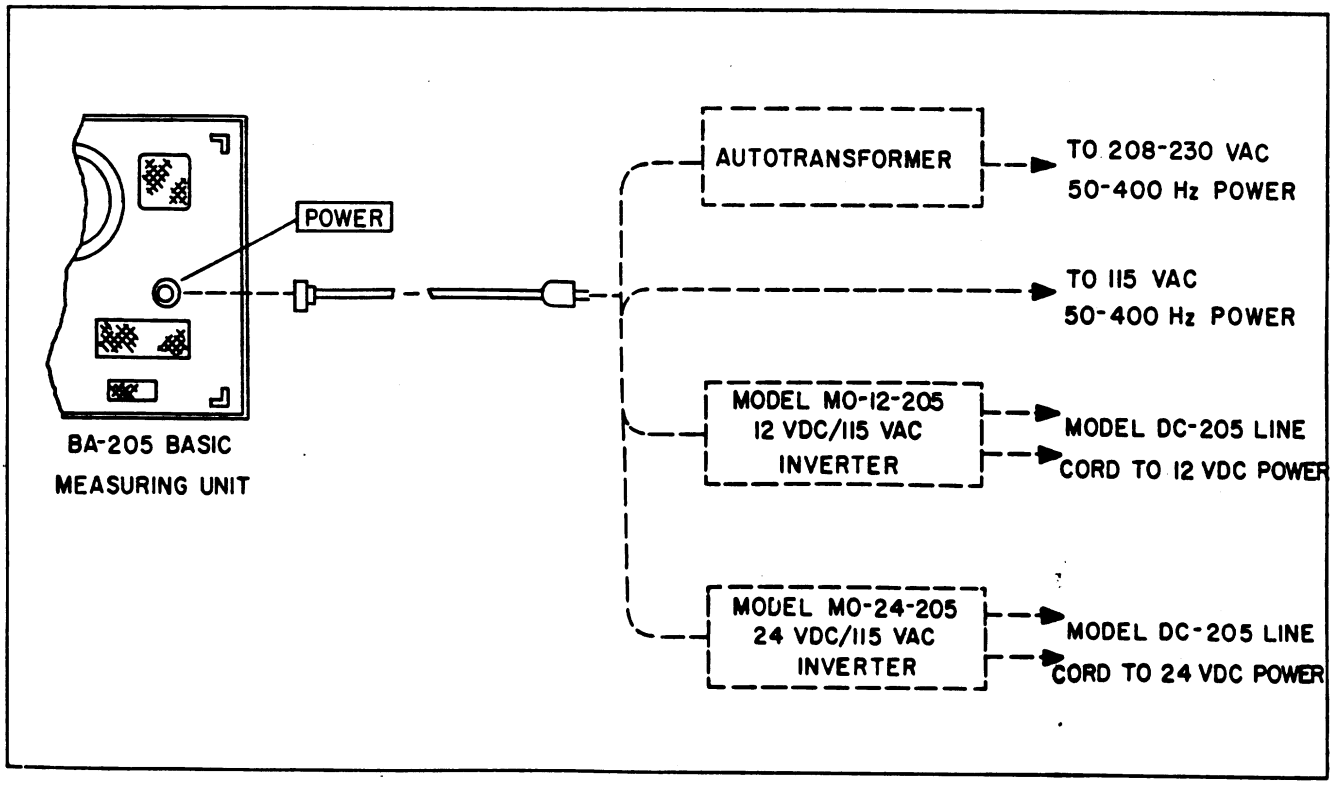

FIGURE A-2: POWER CONNECTION DIAGRAM

3. Quasi-Conductive Measurements. To make quasi-conductive measurements attach the 3-3/4" loop to the surface of the wire of interest (ignition wire or auxiliary electrical wire). The plane of the loop should be parallel to the wire at the point of contact to ensure maximum response from the loop. To ensure that only interference from one wire is being detected all other wires should be displaced at least 6 inches or so from the wire-loop contact point if possible. The cable that interconnects the loop probe and the NF-205 may be dressed, either down under the car if the hood is to be closed or out over the fender. Placement did not appear to be critical.

4. Near-Field Radiation Measurements. To make near-field radiation measurements attach the 3-3/4" loop to a non-conductive tripod at the desired location of the vehicle under test. In the measurements the loop was positioned within a foot or so from the vehicle body. These measurements may also be made within the engine compartment with the loop placed in the area of interest.

When making near-field radiation measurements the plane of the loop should be oriented for maximum response or for the polarization of interest.

b. Set the SIGNAL ATTENUATOR DB switch to 0 SUBST ONLY.

c. Set the BAND SELECTOR switch to the lowest frequency band and rotate the TUNING control counterclockwise to obtain a MHz dial indication corresponding to the low-frequency end of the selected band or to the frequency of interest.

d. Set the Function Selector switch to PULSE PEAK and adjust the GAIN control to obtain an output meter pointer noise indication of 4 on the DECIBELS scale.

e. Set the CAL switch to SERIES. (If the signal frequency is known continue at step k.)

f. Slowly rotate the TUNING control clockwise to scan the band in search of the presence of a broadband signal. Signal interception will cause the output meter pointer to rise upscale above noise as the signal enters the equipment passband.

g. Continue rotating the TUNING control clockwise until a maximum output meter pointer deflection is obtained. Should the output meter pointer deflect to an off-scale indication before reaching a maximum set the SIGNAL ATTENUATOR DB switch to 20.

h. Continue rotating the TUNING control clockwise (inserting r-f attenuation as necessary by means of the SIGNAL ATTENUATOR DB switch) until a maximum output meter pointer deflection is obtained. Note the frequency at which this maximum occurs and the setting of the SIGNAL ATTENUATOR DB switch.

i. Continue rotating the TUNING control clockwise. The output meter pointer will start to drop downscale after the maximum intensity point of the broadband signal leaves the equipment bandpass. Remove r-f attenuation by means of the SIGNAL ATTENUATOR DB switch, while simultaneously rotating the TUNING control, until the output meter pointer again indicates noise when in its most sensitive condition or the pointer once again rises upscale to indicate the interception of another broadband signal.

j. Repeat steps g through i until all broadband signal components within the frequency range of the installed tuning unit have been noted.

k. Tune the equipment to the frequency of interest. Set the attenuator as noted in h (or to a position where the signal is detectable) and set the function switch to METERED SLIDEBACK.

l. Set the SLIDEBACK control fully clockwise.

m. Adjust the VOLUME control to obtain a comfortable aural indication of the signal repetition rate.

n. Carefully rotate the SLIDEBACK control counterclockwise. The intensity of the aural indication will decrease as the control is adjusted. Alternately adjust both the SLIDEBACK and VOLUME controls until the aural indication is just at the threshold of audibility when the VOLUME control is set fully clockwise.

Note

Do not reset the SLIDEBACK control for the remainder of the procedure at the frequency of measurement.

o. Set the CAL switch to SHUNT, set the IMPULSE GENERATOR switch to ON and adjust the IMPULSE GENERATOR DB ABOVE 1μV/MHz switches until the aural indication of the impulse generator repetition rate is just barely at the threshold of audibility. (Note that it may be necessary to reset the position of the SIGNAL ATTENUATOR DB switch. If this is required, note the new setting.)

The intensity of the broadband signal relative to that which it would have been if the loop had a sensitivity equal to that of a $\lambda/2$ dipole, is equal to the sum of: 1) the output level of the impulse generator, 2) the difference between the settings of the SIGNAL ATTENUATOR DB switch for when the broadband signal under measurement is applied and that for when the impulse generator signal is applied, 3) the probe calibration factor (from Figure A-3), and 4) the attenuation due to the length of rf cable used (see manufactures specifications).

Note

If the total insertion loss of the r-f attenuators was reduced to permit the impulse generator output level to reach the threshold of audibility, this difference must be added to the impulse generator output level and cable attenuation. Conversely, if the total insertion loss of the r-f attenuators was increased to permit the impulse generator output level to reach the threshold of audibility, this difference must be subtracted from the sum of the impulse generator output level and the cable of attenuation.

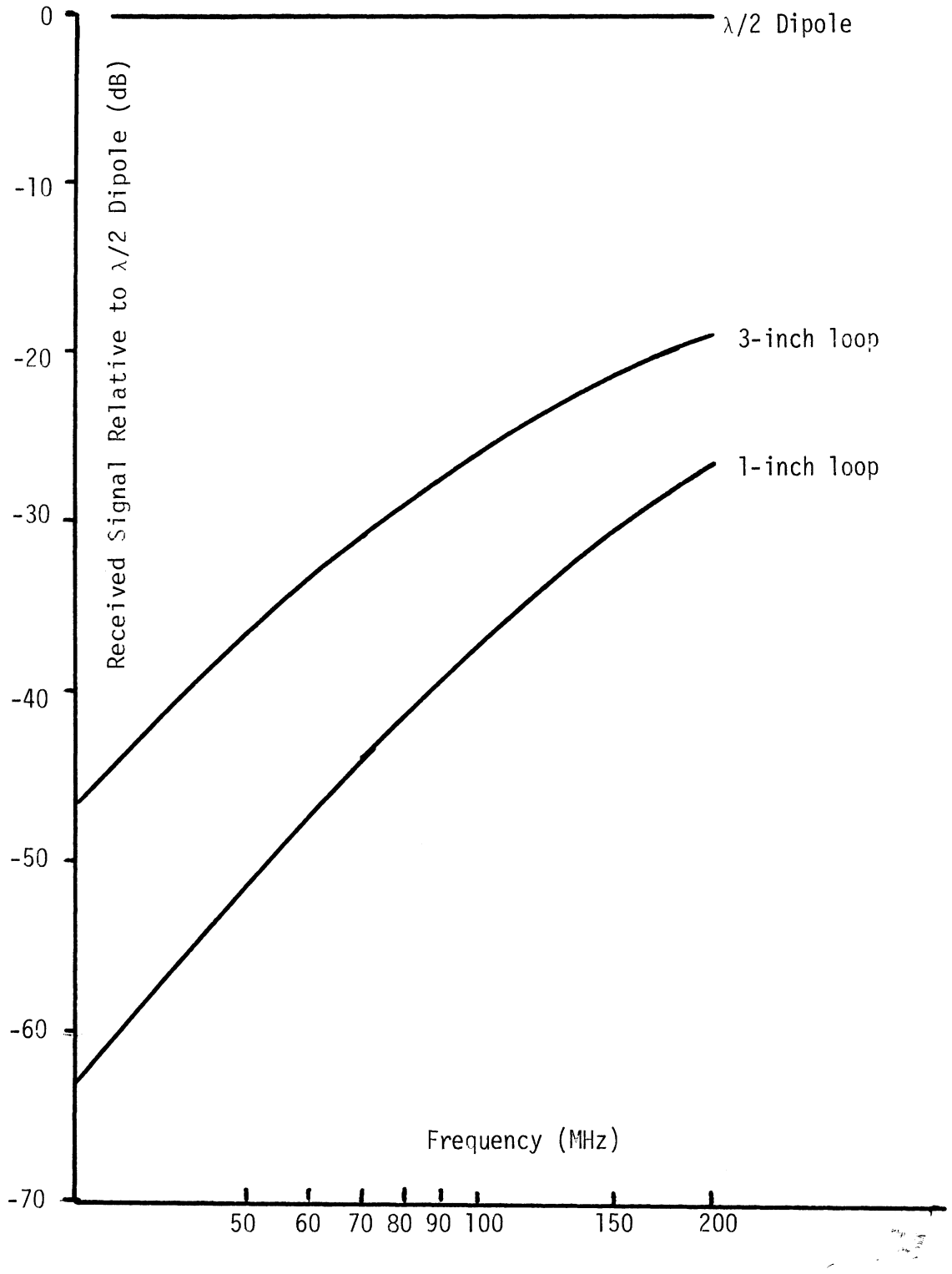

Figure A.3. Probe calibration relative to λ/2 Dipole.

p. De-energize the impulse generator.

q. Repeat steps b through p for the remainder of the frequencies within range of the tuning unit.

V. ACKNOWLEDGEMENTS

The authors are pleased to acknowledge the benefit of several discussions with Mr. Dennis Mullen of the Ford Motor Company. We are grateful for the help provided by Mr. T. Reppucci and Mr. W. Parsons during the measurements. Suggestions and counsel from Professor T.B.A. Senior, Director of the Radiation Laboratory are gratefully acknowledged.

VI. REFERENCES

[1] E. N. Skomal, "Man-Made Radio Noise," Van Nostrand Reinhold Company, New York, pp. 21-74, 1978.

[2] D. F. Herrick, "Investigation of Audio Degradation in Automotive Radio Systems," The University of Michigan Radiation Laboratory Final Report, No. 320674-1-F, June 1977.

[3] J. E. Ferris, R. E. Hiatt and S. Panevetos, "Study of Measurement Techniques Applicable to Automotive Ignition Radiation," The University of Michigan Radiation Laboratory Final Report, No. 320296-1-F, July 1973.

[4] W. Johnson, Ford Scientific Laboratories, Private communication, 1979.

[5] B. P. Lahti, "Communication Systems," John Wiley and Sons, Inc., New York, pp. 30-40, 1968.

[6] V. V. Liepa, "Sweep Frequency Surface Field Measurements," The University of Michigan Radiation Laboratory Final Report 013378-1-F, AFWL-TR-75-217, 1975.

[7] J. D. Kraus, "Antennas," McGraw-Hill Book Co., Inc., N.Y., p. 481, 1950.

[8] King, W. P., Mack, R. B. and Sandler, S. S., "Arrays of Cylindrical Dipoles," Cambridge University Press, p. 372, 1968.